Adjuvant and immunomodulatory potential of Natural Killer T (NKT) activation by NKTT320

Nell G. Bond[1], Marissa Fahlberg[1], Shan Yu[1], Namita Rout[1], Dollnovan Tran[1], Taylor Fitzpatrick-Schmidt[1], Lesli Sprehe[1], Elizabeth Scheef[1], Joseph C. Mudd[1], Robert Schaub[2] and Amitinder Kaur[1*]

[1]Tulane National Primate Research Center, Covington, LA, USA

[2]RGS Consulting, Pelham, NH, USA

*Corresponding Author:

Email: akaur@tulane.edu (AK)

Conflict of interest statement: Dr. Robert Schaub's former employment with NKT Therapeutics, the manufacturer of NKTT320, may be considered a potential conflict of interest.

Abstract

Invariant natural killer T-lymphocytes (iNKT) are a unique subset of immunomodulatory innate T-cells with an invariant TCRα chain recognizing glycolipids presented on the MHC class-I-like CD1d molecule. Activated iNKT rapidly secrete pro-and anti-inflammatory cytokines, potentiate innate and adaptive immunity, and modulate inflammation. While iNKT activation by glycolipid agonists are being explored as an adjuvant, their use depends on CD1d-restricted antigen presentation. Here, we report the effects of iNKT activation by a novel humanized monoclonal antibody, NKTT320, that binds to the invariant region of the iNKT TCR. A single dose of NKTT320 led to rapid iNKT activation, increased polyfunctionality, and elevation of multiple pro-inflammatory and chemotactic plasma analytes within 24 hours in cynomolgus macaques. Flow cytometry and RNA-Seq confirmed downstream effects of NKTT320 on multiple immune cell subsets. Inflammatory response, JAK/STAT and PI3K/AKT pathway genes were enriched along with upregulation of the inflammation-modulating genes CMKLR1, ARG2 and NLRP12. Finally, NKTT320 induced iNKT trafficking to adipose tissue and did not cause iNKT anergy. Our data indicate that NKTT320 has a sustained effect on *in vivo* iNKT activation, potentiation of innate and adaptive immunity, and resolution of inflammation, properties that support its future application as an immunotherapeutic and vaccine adjuvant.

Introduction

Invariant Natural Killer T (iNKT) lymphocytes are rare, innate T-lymphocytes with unique antigen recognition and immunomodulatory properties that make up approximately 0.01-0.1% of circulating T-lymphocytes in humans (1). iNKT were first discovered in mice during anti-tumor studies and named for the expression of the natural killer (NK) marker NK1.1 on T-lymphocytes. iNKT differ from classical T-lymphocytes in multiple distinct, important ways. iNKT express a conserved T-cell receptor (TCR) Vα chain with an invariant complementary determining region 3 (CDR3α) as opposed to the polymorphic TCR on classical T-lymphocytes. Primate iNKT express Vα24-Jα18 which preferentially pairs with a restricted repertoire of Vβ subunits, generally Vβ11 (2). In contrast to classical T-lymphocytes, iNKT recognize and are rapidly activated by both endogenous and exogenous glycolipid antigens presented by antigen presenting cells (APCs) on nonpolymorphic MHC-class-I-like CD1d molecules. The classical, most widely studied iNKT activating lipid antigen is alpha-galactosylceramide (αGC), derived from the marine sponge *Agelas mauritianus* and first identified in murine cancer studies (1). Upon activation, iNKT rapidly produce a wide range of cytokines covering T-helper (Th) 1, Th2 and Th17 functionality, often from the same cell (3). iNKT in primates are more strictly defined by co-staining of the αGC-loaded CD1d tetramer (CD1dTM) and Vα24 on $CD3^+$ T-lymphocytes (4, 5).

Due to their rapid response and broad functional potential, iNKT bridge the gap between innate and adaptive immunity (6). Once activated, iNKT can be directly cytolytic (through perforin and granzyme B) and display Th1, Th2 and Th17 effector functions. Additionally, iNKT rapidly influence the function of multiple immune subsets

(6). Bidirectional interactions between iNKT and dendritic cells (DC) enhances DC maturation and facilitates antigen cross-presentation and priming of antigen-specific T-lymphocyte responses (7, 8). Activated iNKT can potentiate macrophage phagocytic function and affect polarization (6). IFNγ production by iNKT rapidly activates natural killer (NK) cells improving cytolysis (9). Finally, iNKT are known to recruit and provide help to B-cells, improving B-cell maturation, antibody class-switching and overall humoral immunity (10, 11). Due to their diverse immunomodulatory properties, there is great interest in harnessing iNKT activation as an immunotherapeutic tool and a vaccine adjuvant.

Studies exploring αGC-mediated iNKT activation as a vaccine adjuvant have largely been conducted in mice with varying degrees of success (12-16). One barrier to the use of iNKT activating agents such as soluble αGC *in vivo* is subsequent iNKT anergy in which iNKT are rendered unable to respond to further stimuli (17, 18). Although administration of αGC loaded on autologous DCs has shown promise for cancer immunotherapy in human studies (19-21), there is a need for alternate strategies of *in vivo* iNKT activation that can effectively harness the immunomodulatory properties of iNKT for widespread therapeutic use.

Antibodies directed against the iNKT cell receptor are one such class of potential alternative iNKT modulating agents. NKTT120 is a humanized monoclonal iNKT depleting antibody developed by NKT Therapeutics (Sharon, MA) that directly binds to the CDR3 region of the Vα–subunit of the semi-invariant iNKT TCR with high affinity (22). NKTT120 was engineered with an IgG1 Fc, thus supporting Fc-receptor binding and iNKT depletion by antibody dependent cellular cytotoxicity (ADCC) (22).

NKTT120 successfully depleted iNKT without any adverse effects in healthy humans and macaques (22, 23). The humanized monoclonal antibody NKTT320 developed by NKT Therapeutics shares the variable region and iNKT binding specificity with NKTT120 but was engineered with an IgG4 Fc (22) allowing it to successfully bind and activate iNKT without ADCC-mediated depletion (24, 25).

In this study, we characterized the *in vivo* effects of NKTT320 administration on iNKT function and bystander lymphocyte subsets in Mauritian-origin cynomolgus macaques (MCM). We show rapid induction of iNKT activation and polyfunctionality without anergy, downstream effects on monocytes, T- and B-lymphocytes, and gene enrichment in the inflammatory response, heme metabolism, JAK/STAT signaling and PI3K/AKT pathways. Our results demonstrate the utility of NKTT320 as an *in vivo* immunomodulatory tool and a potential novel vaccine adjuvant.

Results

NKTT320 specifically activates iNKT

To characterize the potential of NKTT320 as an adjuvant, we first conducted *in vitro* studies in unfractionated peripheral blood mononuclear cells (PBMCs) of MCM. MCM were chosen because their circulating iNKT frequencies and phenotype are similar to humans (26). As previously reported, iNKT were identified by flow cytometry as T-lymphocytes co-expressing the Vα24 TCR and binding to αGC-loaded CD1d-tetramers (CD1dTM) (5, 26) (Figure 1A, Supplemental Figure 1). PBMCs stimulated *in vitro* with goat-anti-mouse-IgG (GAM-IgG) cross-linked NKTT320 at 200ng/mL showed specific iNKT activation as evidenced by CD3 downregulation, CD69 upregulation, and secretion of IFNγ and TNFα compared to media alone (Figure 1B). Escalating concentrations of NKTT320 showed a dose-dependent effect on iNKT activation as indicated by downregulation of Vα24, CD1dTM, and CD3 (Figure 1C-D). At higher doses, a combination of TCR downregulation and competition for the same invariant TCR binding site resulted in loss of sensitivity to detect CD1dTM-positive iNKT (Figure 1C). iNKT activation was not associated with non-NKT T-lymphocyte activation during a 24-hour stimulation period demonstrating the iNKT specificity of NKTT320 (Figure 1B, D).

We then evaluated *in vitro* NKTT320 treatment for differences in activation of single positive CD4 or CD8 iNKT. Unstimulated cultured $CD4^+$ and $CD8^+$ iNKT did not differ in baseline activation levels measured by surface CD69 and HLA-DR expression (Figure 1E and data not shown). NKTT320 treatment led to significant activation of both $CD4^+$ ($p=0.0312$) and $CD8^+$ iNKT ($p=0.0312$) as measured by CD69 upregulation

(Figure 1E). There was no significant difference in activation of $CD4^+$ compared to $CD8^+$ iNKT (Supplemental Figure 2).

To examine broader functional changes resulting from NKTT320 treatment we cultured PBMC *in vitro* for 48 hours with either media alone (mock stimulation) or with cross-linked NKTT320 and measured secreted analytes using a non-human primate (NHP) 29-plex Luminex (Figure 1F). Eight analytes significantly elevated in the NKTT320-treated supernatants included proinflammatory and Th1 cytokines (IFNγ, TNFα, IL-12, IL-2, IL-15), chemokines (CCL4), and growth factors (FGF-basic, HGF). IL-6, CXCL8 (IL-8), CCL2, CCL3, and CCL5 (RANTES) trended higher but the increase did not reach statistical significance (Figure 1F).

Differential iNKT activation with NKTT320 and αGC stimulation

Since glycolipid agonists are being used for iNKT activation, we compared NKTT320 to the classic iNKT agonist, αGC. In a series of time course *in vitro* stimulation experiments, all parameters of iNKT activation (CD69, IFNγ, TNFα, IL-2 and IL-4) appeared more rapidly and were of greater magnitude after NKTT320 as compared to αGC stimulation (Figure 2A). Increased IFNγ and TNFα secretion, and increased iNKT polyfunctionality were apparent within 4 hours of NKTT320 stimulation (Figure 2A-B). With the exception of IL-4, αGC-stimulated iNKT were able to match responses from NKTT320-stimulated cells by 48 hours (Figure 2A). The kinetic and qualitative differences in iNKT response between NKTT320 and αGC stimulation has implications for therapeutic choice of NKT agonist.

NKTT320 Pharmacokinetics

After determining the effectiveness and specificity of iNKT activation with NKTT320, we set out to determine the pharmacokinetics of this antibody following *in vivo* administration. Dose escalation experiments were performed in three groups of MCM administered a single IV dose of NKTT320 at low (100μg/kg, n=5), mid (300μg/kg, n=3) and high (1000μg/kg, n=3) concentrations. These doses were selected based on previously published data of NKTT120 (22, 23). No adverse effects were observed following *in vivo* NKTT320 administration. Peak serum NKTT320 levels ranging between 5.94-77.46μg/mL were reached within 24 hours of a single IV dose. The iNKT TCR saturation level previously determined for NKTT120 on a Biacore assay against the immobilized iNKT TCR resulted in a K_D of 44nm corresponding to a saturation level of 6μg/mL (22). All NKTT320-treated animals in the high-and mid-dosing groups reached peak levels above the NKT TCR saturation level (6μg/mL) within 30 minutes of antibody administration while 4 of five animals in the low dose (100μg/kg) surpassed TCR saturation levels within 2 hours of administration (Figure 3A).

The kinetics of circulating NKTT320 showed animal to animal variation. Peak NKTT320 serum levels trended higher in the high dose group but did not reach significance (Figure 3A and data not shown). Plasma NKTT320 levels declined below detection in all animals 2-6 weeks post treatment, excepting one animal in the high dose group that maintained detectable serum NKTT320 levels through week 14. NKTT320 plasma concentrations in the high dose group were used to determine the half-life of NKTT320 (Figure 3B). The calculated half-life of 6.81 days or 163.2 hours post

administration is less than the half-life of NKTT120 but consistent with variation in plasma clearance of human IgG antibodies in NHPs (22, 27).

One multiply dosed animal with successive NKTT320 doses administered at two-week intervals (dose 1=30μg/kg, dose 2=100μg/kg and dose 3=100μg/kg) reached the 6μg/mL NKT TCR saturation level only after the second and third dose indicating that the first dose was not sufficient to surpass TCR saturation (data not shown). Multiple doses were additive in this animal and again peaked within 24 hours after each administration (data not shown). These limited data suggest that doses above 30μg/kg NKTT320 are needed for TCR saturation.

NKTT320 effect on iNKT after *in vivo* administration

We monitored *in vivo* changes in iNKT and non-iNKT ($V\alpha24^-$) T-lymphocytes from 30 minutes onwards following a single intravenous dose of NKTT320 (Figure 4). Similar to *in vitro* stimulation (Figure 1A-D), *in vivo* NKTT320 resulted in downregulation of Vα24 TCR and CD1dTM-positive iNKT-cells within 24 hours of administration (Supplemental Figure 3A). Because NKTT320 binds to the invariant region of the NKT TCR, the decrease in CD1dTM-positive iNKT could represent a 'masking' effect. However, the attendant downregulation of Vα24 TCR and CD3 (data not shown) indicates that the decline in detectable Vα24/CD1dTM co-expressing iNKT following NKTT320 administration was also a result of *in vivo* NKT activation. Due to the loss of visualization of $V\alpha24^+CD1dTM^+$ iNKT we also enumerated total $V\alpha24^+$ T-lymphocytes to monitor changes in circulating iNKT frequency post NKTT320 administration (Supplemental Figure 3B).

Both Vα24/CD1dTM co-staining iNKT and total Vα24$^+$ T-lymphocyte frequencies declined significantly after NKTT320 administration (Supplemental Figure 3B). While Vα24/CD1dTM co-staining iNKT frequency was reduced by day 1 and remained significantly lower than baseline through week 14 ($p<0.05$ at all sampled time-points), a significant decline in total Vα24$^+$ T-lymphocyte frequency was only observed for one week post NKTT320 administration. The decline in Vα24$^+$CD1dTM$^+$ iNKT, likely the result of a masking effect, persisted well beyond the time that serum NKTT320 levels were undetectable. This may mean that iNKT-bound NKTT320 undetectable in the blood is slowly released in the tissues and continues to activate iNKT.

Monitoring of HLA-DR and CD69 surface expression revealed rapid, sustained iNKT-specific activation without general T-lymphocyte activation following NKTT320 administration (Figure 4A). By 30 minutes, iNKT were significantly activated above baseline levels ($p=0.0156$) while non-iNKT (Vα24$^-$) T-lymphocytes were not activated. iNKT then remained significantly activated for 6 weeks after treatment. Non-iNKT T-lymphocytes showed a transient significant increase in HLA-DR or CD69 expression post NKTT320 treatment. Activation levels of circulating iNKT remained significantly above non-iNKT T-lymphocytes starting within 30 minutes of NKTT320 administration ($p=0.0039$) and persisted for at least 14 weeks ($p=0.0391$).

To distinguish responses of iNKT subsets, we investigated differences in CD8$^-$ and CD8$^+$ iNKT activation. Both subsets were significantly activated within 30 minutes of NKTT320 administration; while CD8$^-$ iNKT remained significantly activated through week 6 post treatment, increased CD8$^+$ iNKT activation lasted two weeks (Figure 4B). In

contrast to in vitro data, circulating $CD8^-$ iNKT were significantly more activated compared to $CD8^+$ iNKT pre- and post NKTT320 administration ($p=<0.01$).

NKTT320 rapidly modulates T-lymphocyte function

Central to investigation of NKTT320's utility as an adjuvant is its effect on other immune cell subsets. We used intracellular cytokine staining (ICS) flow cytometry to evaluate NKTT320-induced functional changes in mitogen responsiveness of iNKT and non-iNKT T-lymphocytes at discrete time-points after IV NKTT320 administration. Increased responsiveness of iNKT to overnight PMA/ionomycin stimulation was observed within 30 minutes of NKTT320 administration (Figure 5A). A significant increase in IL-2 secretion detected at 30 minutes post NKTT320 was sustained through day 14 post treatment. Likewise, IL-4 was significantly upregulated within two hours of NKTT320 treatment. Significant increases in IFNγ and TNFα were observed day 3 onwards. Increased responsiveness to mitogen stimulation was also observed in Vα24$^-$ "non-iNKT" T-lymphocytes but at a later onset suggesting downstream activation of other T-lymphocyte subsets. The increase in cytokine production in both iNKT and non-NKT T-lymphocytes mainly originated from $CD4^+$ T lymphocytes (Supplemental Figure 4 and data not shown).

NKTT320 also rapidly increased iNKT polyfunctionality; by day 1, over 50% of responding iNKT secreted two or more cytokines on mitogen stimulation (Figure 5B). Increased polyfunctionality was less evident in the non-NKT T-lymphocytes. Overall, iNKT were activated rapidly in response to NKTT320 treatment and appear to have also induced changes in the functional potential of non-iNKT T-lymphocytes.

In vivo iNKT activation results in rapid activation of the innate and adaptive immune system

The ability to modulate innate and adaptive immune responses is crucial when identifying promising immune modulatory tools and vaccine adjuvants. To assess the effect on the host immune response we longitudinally measured plasma analytes by Luminex, and monitored changes in immune cell frequency, phenotype and function by flow cytometry after *in vivo* administration of NKTT320.

A significant increase in 21 plasma analytes was detected in the first 72 hours of NKTT320 administration (Figure 6A, Supplemental Table 1). Plasma CCL2, CXCL10 and IL-6 were elevated within 30 minutes reaching peak levels in the first 2 hours (Figure 6B). Significantly elevated analytes that peaked in the first 24 hours included cytokines and chemokines that likely originated from iNKT (IL-2, IL-4, IL-5, IL-6, IL-10, CCL4, CCL5) and from downstream activation of dendritic cells and monocytes/macrophages (IL-12, IL-1β, IL-1RA, CXCL8, CXCL9-11, IL-6, CCL2, CCL22). Interestingly, IFNγ, TNFα and GM-CSF peaked later at 72 hours (Supplemental Table 1) suggesting iNKT and non-iNKT sources such as NK cells and other T-lymphocytes. Of note, the increase in plasma analytes corresponded temporally to the peak of plasma NKTT320 and iNKT-specific activation. The early response was indicative of rapid activation of the innate immune system and included proinflammatory analytes as well as several chemo-attractants crucial for immune cell recruitment of monocytes, granulocytes, NK cells and activated T-lymphocytes (28, 29).

Consistent with the Luminex data, flow cytometry revealed significant changes in circulating monocytes and B-lymphocytes (Figure 7). A significant increase in $CD14^+$ monocytes detected at day 1 post NKTT320 treatment had declined to baseline levels by week 6 (Figure 7A). Increased levels of proliferating $CD20^+$ B-lymphocytes as measured by Ki67 were detected beginning at day 1 ($p=0.0156$) and intermittently thereafter (Figure 7B). These data are consistent with downstream effects of iNKT activation on other immune cell populations. The broad range of cytokines, chemokines and growth factors detected in response to NKTT320 treatment underscores its ability to rapidly activate the innate immune system and potentially serve as a vaccine adjuvant.

RNA-Seq analysis of effects of *in vivo* NKTT320

To further investigate host immune modulation by NKTT320, we performed bulk RNA-Seq analysis on frozen unfractionated PBMC collected at 0, 30 minute, 2-hour, and 24-hour time-points post NKTT320 administration in four MCM with iNKT frequencies ranging between 0.1-10% of circulating T-lymphocytes (Figures 8-9). RNA-Seq analysis revealed significant sequential differential gene expression following NKTT320 treatment. At 30 minutes post NKTT320, there were 104 unique genes differentially expressed, followed by 244 and 740 genes at 2 and 24-hours, respectively (Figure 8A, Supplemental Table 2). Volcano plots showed significant changes in several genes. Notably, the scavenger receptor CD163 exclusively expressed on monocytes and macrophages (30), was significantly upregulated as early as 30 minutes and sustained through 24 hours (Figure 8B and 8C). Concomitantly, CD83 and TNF-Alpha-Induced Protein 3 (TNFAIP3) were significantly downregulated at 24-hours (Figure 8B).

CD83, a member of the immunoglobulin (Ig) superfamily expressed on mature DCs can regulate inflammation by suppressing IL-12 and MCP-1 production (31). Downregulation of TNFAIP3 or A20, an inhibitor of TCR signaling and NF-κB activation (32) was consistent with promotion of an inflammatory response.

Targeted analysis of differentially expressed genes showed elevation of several lymphoid genes related to monocytes, granulocytes, B-cells, T-cells and NK-cells as early as 30 minutes after NKTT320 administration (Figure 8C). Notable among these were upregulation of the following genes: the low affinity inhibitory Fc gamma receptor FCGR2B involved in regulation of antibody production by B-cells and modulation of antibody-dependent effector function of myeloid cells (33); Fc fragment of IgA receptor FCAR present on myeloid lineage cells and mediating phagocytosis and ADCC (34); C-type lectin-like receptor CLEC1B expressed on NK cells (35); CD14, CD163 expressed on monocytes and macrophages; IL-13 receptor alpha-1 chain (IL13RA1) involved in activation of JAK1, STAT3 and STAT6 induced by IL13 and IL4 (36); the MCP-1 receptor CCR2 mediating monocyte chemotaxis (29); CD40 ligand (CD40L) expressed on iNKT and T-cells promoting DC-iNKT interactions and regulating B-cell function through CD4 help (6); colony stimulating factor 3 (CSF3R) or G-CSF receptor controlling granulocyte maturation and function (37); and N-formyl peptide receptors (FPR1, FPR3) that are powerful neutrophil chemotactic factors (38). Several inflammation-related and pattern-recognition receptor genes were elevated. These included IL1R1; extracellular and cytosolic receptors for bacterial flagellin, namely toll-like receptor 5 (TLR5), and neuronal apoptosis inhibitory protein NAIP that also acts as the sensor component of the NLRC4 inflammasome and promotes caspase-1 activation

(39); the carbohydrate sensing innate immune recognition ficolin FCN1 expressed in monocytes (40); and the C-type lectin receptor CLEC4E or MINCLE expressed on macrophages that recognizes fungal and mycobacterial ligands (41). Upregulation of the chemokine receptor genes CCR2 and CCR1 was concordant with elevated plasma levels of their respective ligands, CCL2 and MIP-1α, post NKTT320 administration (Figure 8 and Supplemental Table 1). Overall, upregulation of these genes was indicative of a broad stimulation of the innate immune system with facilitation of antigen presentation function.

Simultaneously an immune downmodulation effect of NKTT320 was evident by upregulation of several immune inhibitory and inflammation suppressive genes (Figure 8). These included the T-lymphocyte inhibitor PD-1 ligand 1 (CD274) (42); the arginine metabolism enzyme ARG2 that can regulate inflammation and immunity (43-46); the potent mitigator of inflammation, nucleotide-binding oligomerization domain protein NLRP12 that acts as a negative regulator of NF-κB and promotes degradation of NOD (47); the chemerin chemokine-like receptor CMKLR1 which binds the endogenous lipid mediator Resolvin E1 and actively regulates resolution of acute inflammation (48), the suppressor of cytokine signaling SOCS3 involved in the negative regulation of cytokines such as IL6 that signal through the JAK/STAT pathway (49), and ROR1 that can inhibit the Wnt3a-mediated signaling pathway (50). These data point to an inflammation suppressive effect of NKTT320-mediated iNKT activation acting in concert with activation of B-cells, monocytes, dendritic cells, and T-helper pathways. It is noteworthy that both activating and suppressive effects were detected in the first 24-hours of

NKTT320 administration. The inhibitory signals may reflect a feed-back loop following initial activation.

Downregulation of genes such as PRF1, NCR1, GNLY, GZMB, GZMH, CD244 associated with T-lymphocyte and NK cytotoxicity (Figure 8) was unexpected due to the functional evidence for T-lymphocyte activation. Of these, CD244 or 2B4, which belongs to the signaling lymphocyte activation molecule (SLAM)-receptor family and is expressed on NK cells, as well as on some T-cells, monocytes and basophils, can serve as both an activating and inhibitory receptor (51).

We followed the targeted gene analysis with an unbiased analysis of differentially expressed genes post NKTT320 administration. Using Gene Set Enrichment Analysis against four pathway databases, an aggregate of 201, 332, and 423 enriched pathways were detected at 30 minutes, 2 hours and 24 hours respectively post NKTT320 administration (Supplemental Tables 3-4). Normalized enrichment scores of 10 biological pathways related to NKT-lymphocytes that were significantly altered on NKTT320 administration along with heatmaps of genes in these pathways reaching a significant threshold are shown (Figure 9A-B). Because of CD163 upregulation and upregulation of genes involved in phagocytosis we also evaluated genes in the scavenger receptor activity pathway (Figure 9C).

Several genes from the inflammatory response, heme metabolism, neutrophil degranulation, IL-6/JAK/STAT3, and PI3K/AKT pathways were increased within 24 hours of NKTT320 (Figure 9B). Among the upregulated genes, elevation of the CLEC9A gene in the carbohydrate binding pathway was noteworthy. Targeting antigens to the C-type lectin CLEC9A on DCs can induce strong humoral immunity and T follicular helper

responses independent of adjuvant and is being explored as a vaccine strategy (52, 53). Upregulation of the heme metabolism pathway SDCBP gene encoding the syndecan binding protein or syntenin-1 is interesting as it regulates TGFβ1-mediated downstream activation (54).

Downregulated genes in the pathway analysis included the cyclin family gene CCND3, platelet-derived growth factor PDGFB, PIK3CB, and LPAR1, a member of the G protein-coupled receptor superfamily with diverse biological functions including proliferation and chemotaxis. The functional effects of genes that were downregulated appeared to be both pro-activation as well as anti-inflammatory. Several of the downregulated genes in the TNFA signaling pathway were inhibitors of NF-κB activation and it is likely that their suppression would lead to increased activation. Examples include suppression of TNFAIP3 and ZC3H12A, an IL-1-inducible gene encoding the monocyte chemotactic protein-1-induced protein-1 (MCPIP1) that acts as a transcriptional activator but also suppresses NF-κB activation (55). Similarly, suppression of the sphingosine kinase 1 gene (SPHK1) has been shown to potentiate induction of RANTES (56). The clock gene PER1 regulates pro-inflammatory mediators, and its suppression can lead to increased CCL2 and IL6 (57). On the other hand, downregulation of PIK3CB or PI-3 kinase subunit beta in the PI3K/AKT pathway can be instrumental in suppressing inflammation by prevention of AKT phosphorylation and inducing FOXO activation (58).

iNKT maintain proliferative ability and avoid anergy following NKTT320 treatment

One hurdle to therapeutic modalities of *in vivo* iNKT activation is the induction of iNKT anergy. Administration of soluble αGC *in vivo* results in rapid iNKT activation followed by subsequent iNKT anergy in response to further stimulation (18). To test whether *in vivo* NKTT320 treatment induces anergy, we performed *in vitro* proliferation assays in PBMC from NKTT320-treated animals, measuring Ki67 and BrdU double-positive cells after a 6-day stimulation with αGC. iNKT of animals that had received NKTT320 did not display anergy. On the contrary they were more responsive to *in vitro* αGC stimulation and showed increased proliferation compared to a pre-NKTT320 time-point (Figure 10A). Furthermore, iNKT-cells continued to expand in culture on αGC stimulation pre- and post NKTT320 treatment providing further evidence that the monoclonal antibody does not induce iNKT anergy (Figure 10B). The increased *in vitro* iNKT expansion was specific to αGC stimulation and not seen with other stimuli (Supplemental Figure 5). These results were reproducible at day 1 post NKTT320 in 3 of 5 animals assessed by proliferation assays (data not shown). In the single multiply dosed animal, iNKT proliferative ability temporally followed increases in NKTT320 plasma concentration after each dose (Figure 10C). Finally, we saw a comparable or greater increase in plasma IL1RA, IL-6 and MCP-1 after a second dose of NKTT320, providing further evidence for absence of anergy (Figure 10D).

Increased iNKT frequency in adipose tissue after NKTT320 administration

Our observations on the effect of NKTT320 were thus far confined to the examination of peripheral blood where we did not detect an increase in iNKT frequency. To investigate trafficking or effect on tissue iNKT, we examined iNKT frequency pre-and

14 days post-NKTT320 administration in lymph node (LN), bone marrow (BM), bronchoalveolar lavage (BAL), rectal mucosa (REC) and adipose tissue in a subset of animals. Adipose tissue is known to be a site of iNKT localization in humans (59). Interestingly, we observed an increased frequency of adipose iNKT while iNKT frequency at other tissue sites was unchanged (Figure 11A-B). This suggests that either adipose-resident iNKT proliferate in response to NKTT320 treatment or iNKT are trafficking to adipose tissue following NKTT320 treatment.

Discussion

This study is the first demonstration of sustained *in vivo* iNKT activation using the novel iNKT-activating humanized monoclonal antibody, NKTT320, that selectively binds with high affinity to the invariant NKT TCR in humans (25). We used the nonhuman primate model of MCM to extensively characterize the *in vitro* and *in vivo* effects of NKTT320 and assess its utility as an adjuvant and immunomodulatory tool. *In vitro*, NKTT320 showed dose-dependent iNKT-specific activation and increased cytokine production. *In vivo*, a single intravenous inoculation of NKTT320 was sufficient to rapidly induce iNKT activation that was sustained for up to 6 weeks without causing anergy. NKTT320-induced iNKT activation was associated with downstream activation of non-NKT immune cell subsets and iNKT trafficking to or proliferation within adipose tissue. Even though iNKT accounted for only 0.1-10% of circulating T-lymphocytes, iNKT activation had a profound amplification effect due to downstream effects on a wide range of immune cells. Our findings on iNKT activation and downstream effects on $CD4^+$ T-lymphocytes, monocytes, dendritic cells and B cells, make NKTT320 a promising candidate for immunotherapy and vaccine adjuvant.

NKTT320 led to iNKT-specific activation within 30 minutes of administration and was accompanied by increased iNKT polyfunctionality with Th1 and Th2 cytokine secretion, increased proliferative capacity and trafficking to adipose tissue. A greater stimulatory effect on $CD4^+$ iNKT was observed as they were the major source of the cytokines contributing to increased polyfunctionality in mitogen-stimulated iNKT. An increase in IL-2 and IL-4 was followed by IFNγ and TNFα production. IL-2 and IL-4 are both known to regulate and promote T-cell differentiation into Th1 and Th2, respectively.

Additionally, lymph node iNKT secreting IL-4 were recently shown to be a key mediator of humoral immunity, improving B-cell maturation and differentiation as well as antibody class switching (60, 61). Early increases in iNKT function were followed from day 3 onwards by increased cytokine secretion from non-iNKT T-lymphocytes, most notably IL-2, IL-17 and IL-22. Looking beyond the adjuvant potential of NKTT320, these Th17 cytokines are of particular interest in the context of HIV infection as they are known to play a major role in maintaining gut mucosal integrity.

NKTT320-induced activation had features that were distinct from glycolipid iNKT agonists. While NKTT320 activated iNKT within two hours of stimulation and reached peak response levels by 16 hours, αGC stimulation was slower to catch up requiring 48 hours to reach comparable levels. Additionally, NKTT320 resulted in a broader Th1 and Th2 response whereas αGC skewed towards Th1 alone. Whether this holds true *in vivo* remains to be seen. Few *in vivo* studies of iNKT activation using αGC in humans and macaques have described functional changes by ICS in response to mitogen stimulation. When described, increases in Th1 cytokine production, primarily IFNγ were reported (62). Although synthetic sphingolipid NKT agonists that drive Th2 responses are available (63), NKTT320 may be advantageous because it fosters an environment of increased responsiveness directing polyfunctional responses to specific stimuli without the need for structural modifications. Furthermore, NKTT320 does not rely on CD1d-mediated antigen presentation for iNKT activation. This could be an advantage in disease settings such as tumors and HIV infection associated with CD1d downregulation. Another major advantage of NKTT320 is the absence of NKT anergy. Following *in vivo* treatment with αGC, iNKT rapidly become anergic and are unable to

441 respond to further stimuli-either iNKT specific or general TCR stimulation (18). The ideal
442 tool for *in vivo* iNKT modulation would transiently activate iNKT while avoiding anergy.
443 The fact that *in vivo* NKTT320 activates iNKT in the absence of anergy further
444 underscores the promising nature of this antibody as an effective tool for *in vivo* immune
445 manipulation.

446 Circulating iNKT frequencies were transiently reduced post NKTT320, which is
447 consistent with previous studies of *in vivo* iNKT activation using αGC in pig-tailed
448 macaques and humans (62, 64, 65). It is important to consider that the decrease in
449 circulating iNKT frequency could be the result of a masking effect due to NKTT320
450 binding to the same site as CD1dTM, or to activation and subsequent downregulation of
451 the iNKT TCR rendering it difficult to detect iNKT. Another explanation is that iNKT
452 trafficking to tissue effector sites after activation could also transiently decrease the
453 frequency of circulating iNKT. Our observation of elevated iNKT frequencies in adipose
454 tissue following NKTT320 treatment suggests this possibility. This is an interesting
455 finding as adipose tissue has been recently recognized as an inflammatory site with
456 significant involvement in metabolic syndromes (66). Additionally, adipose tissue is a
457 known site of HIV/SIV reservoir (67). The ability of NKTT320 to induce either
458 proliferation or trafficking of iNKT to adipose tissue has implications for use in targeting
459 the HIV/SIV reservoir. Further investigation of the tissue effects of NKTT320 are
460 warranted.

461 Due to the unique regulatory function of iNKT-cells, iNKT activation influences
462 downstream immune cells. Through multiple lines of evidence based on flow cytometry,
463 Luminex and RNA-Seq data, we show profound and broad effects of NKTT320 on the

innate and adaptive immune system, particularly on monocytes/macrophages. Increased levels of plasma IL-6, CCL2 and CXCL10 were detected as early as 30 minutes after NKTT320 antibody administration. A significant increase in circulating $CD14^+$ monocyte frequency was observed at day 1 along with rapid upregulation of CD14, CD163 and CLEC4E gene expression within 30 minutes of antibody administration. Additionally, CCR2 (present on activated macrophages) gene expression was significantly upregulated at two hours in concert with significantly elevated plasma levels of its ligand CCL2. These data point to a rapid release of proinflammatory cytokines and chemokines along with mobilization of monocytes and activated macrophages initiated by NKTT320 administration. The downstream effects of NKTT320-mediated iNKT activation also included release of chemo-attractants involved in the recruitment of granulocytes, NK cells, and T-lymphocytes to sites of inflammation. Increase in chemokines involved in granulocyte recruitment included CCL11 (eotaxin) for eosinophil recruitment; CXCL8 (IL8) for neutrophil recruitment; CCL2 (MCP1) chemoattractant for basophils and monocytes; CXCL9-11 for chemoattraction of Th1 CXCR3-expressing T-cells to inflammatory sites; and CCL22 (MDC) chemoattractant for monocytes, DC, NK and T-lymphocytes (28). Surprisingly, several genes in the IFNγ and TNFα signaling pathways and cytotoxic related genes were downregulated despite evidence of elevated plasma TNFα and IFNγ by Luminex. Although unexpected, the transcriptomics data represented a snap-shot of the first 24 hours whereas in the Luminex we saw plasma levels of TNF-α and IFN-γ peak only at 72 hours. mRNA and protein expression levels are often discordant for the same time-point during dynamic

transitions, as was the case in the first 24 hours of NKTT320 administration which likely explains differences in Luminex and RNA-Seq data (68).

Several pattern recognition receptor genes expressed on dendritic cells and monocyte/macrophages were modulated by NKTT320. Notable among them was the C-lectin type receptor CLEC9a which is expressed on DCs and has been shown to efficiently induce humoral immunity and a T follicular helper response when antigen targeted to CLEC9a displays it to B-cells (52, 69). Evidence of early DC activation was manifested by increased plasma IL-12 detection along with increased gene expression for a range of C-lectins associated with APCs. Additionally, gene expression of TLR5, a ubiquitous pathogen recognition marker found on DCs, and NAIP involved in bacterial flagellin recognition were upregulated. CD40 ligand (CD40L) gene expression was also upregulated likely on NKT and other $CD4^+$ T-lymphocytes. A major pathway by which NKT promote DC/APC maturation is by upregulation of CD40L providing co-stimulation to DCs via CD40L and IFNγ, TNFα (6). Moreover, NKT licensing of DCs for antigen cross-presentation can determine the type of the immune response. These data underscore the effect of NKTT320 on APCs which could lead to improved antigen presentation and potentiation of cellular immunity.

In addition to effects on APCs, we found that NKTT320 treatment had downstream effects on B-cells suggesting synergistic effects that likely improve humoral immunity. In the absence of a vaccine allowing a direct readout of humoral immune responses we found several indications of effects of NKTT320 treatment on B-cells. We found that B-cell proliferation was significantly increased, with Ki67 expression on circulating $CD20^+$ B-cells reaching significantly higher levels at day 1 after antibody

administration. Furthermore, increased B-cell proliferation paired with increases in IL-4 expression from iNKT within 2 hours of NKTT320 administration, suggests the potential for this antibody to improve humoral immunity. These findings were corroborated by the rapid upregulation of B-cell related genes FCAR, IGJ and FCGR2B. These data show the potential to harness the effect of iNKT using NKTT320 to improve APC and B-cell function ultimately improving antigen-specific antibody responses in the context of vaccination or infection.

Interestingly, our data show the potential of NKTT320 to modulate both inflammatory and anti-inflammatory responses. As illustrated in the schematic (Figure 12), side-by-side with activation, NKTT320 triggered several genes encoding markers of resolution of inflammation. Most prominent of the upregulated genes included the inflammation resolution genes NLRP12 and CMKLR1 (48, 70), the metabolic regulator ARG-2 (46), and the inhibitory receptors FCGR2B and PD-L1 (33, 42). In all, the concordant immune activation and anti-inflammatory responses induced by NKTT320 may mean that there is a potential *in vivo* for eliciting potent inflammatory responses without excessive or non-resolving immune activation. This remains to be tested in both long-term studies and in the context of vaccination or infection.

In summary, the current studies detailed here investigate the use of NKTT320, an iNKT-specific humanized monoclonal antibody, for *in vivo* iNKT activation for the first time in the NHP model. We found, through multiple modes of investigation, that this antibody directly affects iNKT without inducing anergy and subsequently transactivates other immune subsets, most strikingly monocytes and macrophages. NKTT320 administration induces potent functional changes in both T-cell and non-T-cell subsets

that may influence both innate and adaptive immunity. It also triggers a balanced immune response with induction of anti-inflammatory responses to balance immune activation. The long half-life of NKTT320 as well as detection of effects on iNKT functionality well beyond the duration of detectable plasma NKTT320 indicates that this therapeutic modality would be feasible in human studies or in a translational setting. NKTT320 is a promising iNKT activating agent that should be studied further for efficacy as a vaccine adjuvant and immunotherapeutic tool.

Materials and Methods

Ethics statement for *in vivo* non-human primate studies

In vivo non-human primate studies were performed at New England Primate Research Center (NEPRC) (Boston, MA; 2013-2015) and Tulane National Primate Research Center (TNPRC) (Covington, LA; 2015-2018). This study was carried out in accordance with the Guide for the Care and Use of Laboratory Animals of the NIH. The protocol was reviewed and approved by the Institutional Animal Care and Use Committees (IACUCs) at NEPRC and TNPRC. The facilities also maintained an Animal Welfare Assurance statement with the National Institutes of Health, Office of Laboratory Animal Welfare.

Animals and Study design

We longitudinally evaluated blood from adult male MCM (n=12) and tissues from a subset of these animals (n=3), pre and post NKTT320 treatment.

Single-dose pharmacokinetic studies: NKTT320 was administered by intravenous route at escalating doses in three groups: low (100μg/kg, n=6), mid (300μg/kg, n=3) and high (1000μg/kg, n=3). Samples were taken prior to NKTT320 administration, and 30 minutes, 2 hours, days 1, 3, 7, and weeks 2, 4, 6, 8, and 14 post treatment. Animals were released to the second phase of the study after the final time point.

Repeated dose studies: One animal received 3 doses of NKTT320—30μg/kg, 100μg/kg and 100μg/kg—at 2-week intervals.

Processing of peripheral blood and tissues

Peripheral blood mononuclear cells (PBMCs) were isolated from MCM by density gradient centrifugation. In brief, peripheral blood was diluted 1:1 in PBS and layered over 90% ficoll at a 1:2 ratio. The gradient was then spun at 2,200 rpm for 45 minutes with the brake off. Cells were then isolated, washed and counted according to standard methods. PBMCs were used for phenotyping and functional assays. In a subset of experiments bone marrow (BM), bronchoalveolar lavage (BAL), peripheral lymph node (PLN), rectal mucosa, subcutaneous abdominal adipose tissue biopsies were taken. In brief, tissue lymphocytes were isolated as follows. BM was treated identically to peripheral blood, described above. BAL was strained, spun at 1,500 rpm for 5 minutes and counted. PLN lymphocytes were isolated using mechanical separation. Rectal mucosa lymphocytes were isolated by enzymatic digestion with EDTA followed by collagenase II. Remaining tissue was mechanically disrupted, strained and washed before counting. Similarly, adipose tissue was initially digested using collagenase II followed by mechanical disruption, straining out remaining tissue and washing the cells before counting. Tissue lymphocytes were used to assess iNKT frequency within tissues following activation with NKTT230.

NKTT320 ELISA

NKT Therapeutics developed an enzyme-linked immunosorbent assay (ELISA) to determine NKTT320 concentration in monkey plasma or serum based on the detection of human IgG4. Briefly, 96 well plates were coated with monkey adsorbed goat anti-human IgG (1μg/mL) and incubated at 37°C for 2 hours or 4°C overnight. Plates were washed 3x with wash buffer (0.05% Tween 20 in 1X PBS). Wells were blocked using

3% BSA in 1X PBS for 2 hours at room temperature. Plates were washed as described above, diluted samples, standards and controls were added and incubated for either 2 hours at room temperature or overnight at 4^{o}C. For antibody detection, 0.1μg/mL goat anti-human IgG Biotin (monkey adsorbed) was added to each well and incubated for 1 hour at room temperature. Plates were washed as described above, 100μL diluted streptavidin-HRP polymer (SPP) conjugate was added, and samples were incubated 1 hour at room temperature. Plates were washed as described above, 100μL of Tetramethylbenzidine (TMB) was added to each well, incubated in the dark for between 10-20 minutes and the reaction was stopped by adding 100μL stop solution to each well. Plates were read at 450nm within 30 minutes of adding stop solution on a Biotek synergy 2 (Winooski, VT) microplate reader and data was acquired and analyzed using Gen5 1.11.5 software, Excel and GraphPad/PRISM.

Cells and reagents

CD1d transfectants: C1R cells (5) were used either loaded with αGC (Avanti Polar Lipids; Alabaster, AL) or alone to stimulate PBMC to compare a known iNKT specific stimulant with NKTT320 stimulation. C1R transfectanT-cells were used at a ratio of 1:10 C1R: PBMC for stimulation.

Alpha-galactosylceramide: αGC stock was received at 2mg/mL from Avanti Polar Lipids, Alabaster, AL and stored in 10μL aliquots in brown glass at -80^{o}C. Aliquots of working solution of 20μg/mL in R10 medium (RPMI+Hepes+L-glutamine+10% fetal calf serum) were stored at -20^{o}C until use. αGC was loaded onto C1Rd cells and used for iNKT stimulation at a final concentration of 100ng/mL.

NKTT320 monoclonal antibody: NKTT320 is a humanized monoclonal antibody developed by NKT Therapeutics (Sharon, MA) that binds to the CDR3 region of the Vα chain of the human iNKT TCR (22, 25, 71). NKTT320 is the sister antibody to NKTT120 (22, 23). Briefly CD1d knock out mice, which lack iNKT-cells, were immunized with cyclic peptides from the CDR3 loop of the TCRα and screened for antibodies. One mouse monoclonal antibody designated 6B11, was identified as specific for human and non-human primate but not rodent iNKT-cells. 6B11 has demonstrated the ability to identify, purify, activate and expand iNKT-cells (72). To permit the clinical evaluation the murine mAb, 6B11, was humanized and de-immunized using the "Composite Human Antibody™ Technology" (Antitope Ltd., Cambridge, UK) to a stabilized IgG4 activating antibody NKTT320. NKTT320 was evaluated by Surface Plasmon Resonance (SPR) assays to determine the binding affinity to soluble human iTCR. NKTT320 binds specifically and selectively to the human iTCR with a K_D of approximately 44 nM. Measurement of binding affinity and functional characterization of NKTT320 was performed using recombinant human invariant TCR and cells. NKTT320 was produced by Antitope LTD (Cambridge, UK) in a transfected CHO-M cell line provided by Selexis sa (Chemin des Aulx Switzerland).

Monoclonal antibodies for flow cytometry: Monoclonal antibodies were used for phenotyping and flow cytometric functional assays. Antibody clone, vendor and panel information can be found in Supplementary Table 5.

iNKT Detection

CD1dTMs loaded with αGC conjugated to either APC or BV421 were obtained from the NIH Tetramer core. These loaded tetramers were titrated and used at the optimal titrated volume. iNKTs are identified based on co-expression of CD1d-TM and Vα24 as described previously (5). Briefly, isolated cells were washed, incubated with titrated volumes of CD1dTM at room temperature for 30 minutes followed by addition of the remaining antibodies in the staining cocktail for 20 minutes. Standard flow cytometric protocols were used for the remaining surface or intracellular cytokine staining panels. A minimum of 2 million PBMCs were used for flow cytometric staining to allow for at least 200,000 lymphocyte events to be captured to visualize rare iNKT populations. All flow cytometry panels were run on either BD LSR-II or BD Fortessa instruments (BD, Franklin Lakes, NJ) by the TNPRC Flow Cytometry Core.

In vitro iNKT stimulation

In vitro stimulation with soluble NKTT320: Peripheral blood mononuclear cells (PBMC) isolated from 3 MCM were incubated with escalating concentrations (0.1, 1, 10 and 25ug/mL) of NKTT320 diluted in R10 media (RPMI/1%Hepes/10%FBS). Cells were incubated overnight at 37°C and harvested for Flow Cytometry staining.

In vitro stimulation with cross-linked NKTT320: PBMC were stimulated with 200ng/mL NKTT320 cross-linked with goat-anti-mouse (GAM) IgG Fab2 fragments. Briefly wells were first coated with GAM-IgG at 2.5ng/mL (SeraCare, formerly KPL, Gaithersburg, MD) in 50mM TRIS buffer (pH=8.6), 1mL per well, and incubated for 1 hour at 37°C. Wells were then washed 3x with PBS and 1mL/well 200ng/mL NKTT320 in PBS was added. Plates were then incubated another hour at 37°C, washed and 1 million PBMC

in R10 media were added to each well. Cells were then incubated 48 hours, harvested for flow cytometry; supernatants were harvested for Luminex assay.

In vitro stimulation with αGC: PBMC were stimulated with 100ng/mL αGC loaded onto C1Rd cells. C1Rd cells were irradiated at 10,000 rads (100 Gy) and mixed with PBMCs at a ratio of 1:1000. Finally, 100ng/mL αGC was added and plates were incubated 48 hours. Cells were then harvested for flow cytometry and supernatants were harvested for Luminex assay.

Proliferation Assays

In vitro proliferation assays were conducted to assess iNKT proliferative ability and anergy following multiple *in vivo* doses of NKTT320. PBMC from days 0, 1, 7, 14 following each dose of NKTT320 were assessed. One million PBMC per condition were stimulated with either R10 media, aGC or staphylococcal enterotoxin B (SEB) (Sigma, Saint Louis, MO). Cells were seeded at 0.2M per well in a 96-well plate and brought up to 200μL/well with R10, 100ng/mL αGC or 200ng/mL SEB. Plates were incubated at 37^{o}C for 5-6 days and 10uM Bromo-2'-deoxyuridine (BrdU, vendor) was added to each well 24 hours prior to staining. On the 6-7th day of incubation, cells were pooled by time-point and stimulation condition and analyzed by flow cytometry.

Luminex

Luminex technology was used to assess plasma chemokine and cytokine levels following NKTT320 treatment in 12 MCM. We used the Invitrogen (Carlsbad, CA) magnetic bead Monkey Cytokine Magnetic 29-Plex Panel covering the following

analytes: EGF, HGF, VEGF, MIG, RANTES, Eotaxin, IL-8, GM-CSF, TNF alpha, IL-1 beta, IL-2, IL-4, IL-5, IL-6, IL-10, IL-12, MIP-1 alpha, IL-17, MIP-1 beta, IP-10, IL-15, MCP-1, G-CSF, IFN gamma, FGF-Basic, IL-1RA, MDC, MIF, I-TAC. Final reactions were read on a Bio-Plex® 200 System (Bio-Rad Laboratories, Hercules, CA) results were calculated using Bio-Plex Manager™ Software v6.2 (Bio-Rad) by the TNPRC Pathogen Quantification and Detection Core.

RNA-Seq

Sample preparation for RNA-Seq: RNA was extracted from snap frozen, unfractionated PBMCs using the Qiagen RNeasy Plus Mini Kit (Qiagen 74134). Briefly, cells were first thawed and pelleted, then lysed following the kit protocol. gDNA was removed using a gDNA Eliminator spin column, and remaining flow through was added to a RNeasy spin column to bind RNA. The spin column/RNA was washed, RNA was eluted and stored at -80^{o}C. Later, samples were concentrated using Zymo Clean & Concentrate-5 Kit (R1013). Briefly, RNA was thawed, bound, and added to the Zymo-Spin IC Column. Then RNA bound to the column was washed, eluted, aliquoted and stored at -80^{o}C. Sample concentration was analyzed on the Qubit Fluorometer using the Qubit RNA BR Assay Kit. Samples were analyzed on the Tape Station at the Sequencing Core at CTRII Tulane University to determine RNA integrity number (RIN). Samples were then submitted for RNA-Seq analysis using a high output, and single read 75 cycle run.

RNA-Seq data analysis: RNA-seq for Eukaryotes Analysis v3 was used for sequencing analysis and built by the Banana Slug Genomics Center at the University of California Santa Cruz. First, an Illumina sequencer at the Tulane School of Medicine Genomics

Core was used to construct raw sequencing reads which were checked for quality and contaminants using FastQC (73). Next, Trimmomatic was used to trim adapter sequences and primers from the sequencing reads (74). Removal of polyA tail, polyN, and read segments with a quality score below 28 was accomplished by using PRINSEQ (75). Following trimming, any reads of length less than 20bp were removed. Quality check was repeated, and high-quality reads were then mapped to the GRCh37/hg19 reference genome using STAR (76, 77) with NCBI RefSeq (78) annotated genes transcriptome index data. Raw read counts were normalized across all samples and then used for differential expression analysis using DESeq (79) and edgeR (80) separately. Genes related to the immune system and with p-values of <0.05 from the edgeR pipeline were identified and categorized by major cell type, which were then plotted on individual heatmaps. Heatmaps were constructed using $\log_2$ fold change data and using the 'pheatmap' package in R (81).

Gene Set Enrichment Analysis: GSEA was performed with the R package 'ClusterProfiler' at default parameters. Enrichment scores were calculated against the following 4 pathway databases containing a priori-defined gene sets: Gene Ontology (GO) database, Hallmark (H) and Curated (C2) gene sets of the Molecular Signature database (MsigDB), and WikiPathways. Gene sets significantly enriched in the datasets ($p < 0.05$) were subsequently curated for those relevant to NKT cell biological function. Enrichment plot was generated with the R software package 'ggplot2' and heatmaps with the 'pheatmap' package.

724

725 **Data Analysis**

726 All flow cytometry data were analyzed using FlowJo version 9.9 (Ashland, Oregon).
727 Cytokine polyfunctionality analyses were done using simplified presentation of incredibly
728 complex evaluations (SPICE) (82). Graphs were generated, and t-tests were performed
729 using GraphPad/PRISM (LaJolla, CA). Statistical analyses were performed in
730 GraphPad/PRISM using the non-parametric Wilcoxon Signed Rank test or paired t-test.

Author Contributions:

Designing research studies: AK, NB; conducting experiments: NB, SY, NR, DT, ES, TFS, LS; acquiring data NB, NR, DT, SY, ES, TFS, LS; analyzing data: NB, MF, JM, RS, AK; providing reagents: RS; and writing the manuscript: NB, AK.

Acknowledgments:

We would like to acknowledge TNPRC Veterinary Medicine Staff for caring for the animals, TNPRC Flow Cytometry Core for acquiring flow cytometry data, and the TNPRC Pathogen Detection and Quantification Core for reading and analyzing the Luminex plates. We thank Cathy Flemington and Alanna Wanek in the Tulane Center for Translational Research in Infection & Inflammation NextGen Sequencing Core for technical assistance for the RNA-Seq studies. We would like to acknowledge Dr. Mark Exley for thoughtful discussion. Study was funded by NIH/NIAID R01 AI102693 (AK), R21 AI145642 (AK) and P51 OD011104-55. The authors would like to thank the NIH Tetramer Core facility for provision of the CD1dTM conjugated to both APC and BV421.

References:

1. Berzins SP, Smyth MJ, and Baxter AG. Presumed guilty: natural killer T cell defects and human disease. *Nature reviews Immunology.* 2011;11(2):131-42.
2. Bendelac A, Savage PB, and Teyton L. The biology of NKT cells. *Annual review of immunology.* 2007;25:297-336.
3. Van Kaer L, Parekh VV, and Wu L. The Response of CD1d-Restricted Invariant NKT Cells to Microbial Pathogens and Their Products. *Frontiers in immunology.* 2015;6:226.
4. Watarai H, Nakagawa R, Omori-Miyake M, Dashtsoodol N, and Taniguchi M. Methods for detection, isolation and culture of mouse and human invariant NKT cells. *Nat Protoc.* 2008;3(1):70-8.
5. Rout N, Else JG, Yue S, Connole M, Exley MA, and Kaur A. Paucity of CD4+ natural killer T (NKT) lymphocytes in sooty mangabeys is associated with lack of NKT cell depletion after SIV infection. *PLoS One.* 2010;5(3):e9787.
6. Brennan PJ, Brigl M, and Brenner MB. Invariant natural killer T cells: an innate activation scheme linked to diverse effector functions. *Nature reviews Immunology.* 2013;13(2):101-17.
7. Fujii S, Liu K, Smith C, Bonito AJ, and Steinman RM. The linkage of innate to adaptive immunity via maturing dendritic cells in vivo requires CD40 ligation in addition to antigen presentation and CD80/86 costimulation. *The Journal of experimental medicine.* 2004;199(12):1607-18.
8. Stober D, Jomantaite I, Schirmbeck R, and Reimann J. NKT cells provide help for dendritic cell-dependent priming of MHC class I-restricted CD8+ T cells in vivo. *J Immunol.* 2003;170(5):2540-8.
9. Carnaud C, Lee D, Donnars O, Park SH, Beavis A, Koezuka Y, et al. Cutting edge: Cross-talk between cells of the innate immune system: NKT cells rapidly activate NK cells. *J Immunol.* 1999;163(9):4647-50.
10. Chang PP, Barral P, Fitch J, Pratama A, Ma CS, Kallies A, et al. Identification of Bcl-6-dependent follicular helper NKT cells that provide cognate help for B cell responses. *Nature immunology.* 2011;13(1):35-43.
11. King IL, Fortier A, Tighe M, Dibble J, Watts GF, Veerapen N, et al. Invariant natural killer T cells direct B cell responses to cognate lipid antigen in an IL-21-dependent manner. *Nature immunology.* 2011;13(1):44-50.
12. Kopecky-Bromberg SA, Fraser KA, Pica N, Carnero E, Moran TM, Franck RW, et al. Alpha-C-galactosylceramide as an adjuvant for a live attenuated influenza virus vaccine. *Vaccine.* 2009;27(28):3766-74.
13. Gonzalez-Aseguinolaza G, Van Kaer L, Bergmann CC, Wilson JM, Schmieg J, Kronenberg M, et al. Natural killer T cell ligand alpha-galactosylceramide enhances protective immunity induced by malaria vaccines. *The Journal of experimental medicine.* 2002;195(5):617-24.
14. Fujii S, Shimizu K, Smith C, Bonifaz L, and Steinman RM. Activation of natural killer T cells by alpha-galactosylceramide rapidly induces the full maturation of dendritic cells in vivo

and thereby acts as an adjuvant for combined CD4 and CD8 T cell immunity to a coadministered protein. *The Journal of experimental medicine.* 2003;198(2):267-79.

15. Silk JD, Hermans IF, Gileadi U, Chong TW, Shepherd D, Salio M, et al. Utilizing the adjuvant properties of CD1d-dependent NK T cells in T cell-mediated immunotherapy. *The Journal of clinical investigation.* 2004;114(12):1800-11.
16. Venkataswamy MM, Baena A, Goldberg MF, Bricard G, Im JS, Chan J, et al. Incorporation of NKT cell-activating glycolipids enhances immunogenicity and vaccine efficacy of Mycobacterium bovis bacillus Calmette-Guerin. *J Immunol.* 2009;183(3):1644-56.
17. Fujii S, Shimizu K, Kronenberg M, and Steinman RM. Prolonged IFN-gamma-producing NKT response induced with alpha-galactosylceramide-loaded DCs. *Nature immunology.* 2002;3(9):867-74.
18. Parekh VV, Wilson MT, Olivares-Villagómez D, Singh AK, Wu L, Wang CR, et al. Glycolipid antigen induces long-term natural killer T cell anergy in mice. *The Journal of clinical investigation.* 2005;115(9):2572-83.
19. Kunii N, Horiguchi S, Motohashi S, Yamamoto H, Ueno N, Yamamoto S, et al. Combination therapy of in vitro-expanded natural killer T cells and alpha-galactosylceramide-pulsed antigen-presenting cells in patients with recurrent head and neck carcinoma. *Cancer science.* 2009;100(6):1092-8.
20. Motohashi S, Okamoto Y, Yoshino I, and Nakayama T. Anti-tumor immune responses induced by iNKT cell-based immunotherapy for lung cancer and head and neck cancer. *Clinical immunology (Orlando, Fla).* 2011;140(2):167-76.
21. Chang DH, Osman K, Connolly J, Kukreja A, Krasovsky J, Pack M, et al. Sustained expansion of NKT cells and antigen-specific T cells after injection of alpha-galactosyl-ceramide loaded mature dendritic cells in cancer patients. *The Journal of experimental medicine.* 2005;201(9):1503-17.
22. Scheuplein F, Thariath A, Macdonald S, Truneh A, Mashal R, and Schaub R. A humanized monoclonal antibody specific for invariant Natural Killer T (iNKT) cells for in vivo depletion. *PLoS One.* 2013;8(9):e76692.
23. Field JJ, Majerus E, Ataga KI, Vichinsky EP, Schaub R, Mashal R, et al. NNKTT120, an anti-iNKT cell monoclonal antibody, produces rapid and sustained iNKT cell depletion in adults with sickle cell disease. *PLoS One.* 2017;12(2):e0171067.
24. Reddy MP, Kinney CA, Chaikin MA, Payne A, Fishman-Lobell J, Tsui P, et al. Elimination of Fc receptor-dependent effector functions of a modified IgG4 monoclonal antibody to human CD4. *J Immunol.* 2000;164(4):1925-33.
25. Patel NP, Guan P, Bahal D, Hashem T, Scheuplein F, Schaub R, et al. Cancer Immunotherapeutic Potential of NKTT320, a Novel, Invariant, Natural Killer T Cell-Activating, Humanized Monoclonal Antibody. *Int J Mol Sci.* 2020;21(12).
26. Rout N, Greene J, Yue S, O'Connor D, Johnson RP, Else JG, et al. Loss of effector and anti-inflammatory natural killer T lymphocyte function in pathogenic simian immunodeficiency virus infection. *PLoS pathogens.* 2012;8(9):e1002928.
27. Newman R, Hariharan K, Reff M, Anderson DR, Braslawsky G, Santoro D, et al. Modification of the Fc region of a primatized IgG antibody to human CD4 retains its ability to modulate CD4 receptors but does not deplete CD4(+) T cells in chimpanzees. *Clinical immunology (Orlando, Fla).* 2001;98(2):164-74.

28. Bromley SK, Mempel TR, and Luster AD. Orchestrating the orchestrators: chemokines in control of T cell traffic. *Nature immunology.* 2008;9(9):970-80.
29. Deshmane SL, Kremlev S, Amini S, and Sawaya BE. Monocyte chemoattractant protein-1 (MCP-1): an overview. *J Interferon Cytokine Res.* 2009;29(6):313-26.
30. Moestrup SK, and Moller HJ. CD163: a regulated hemoglobin scavenger receptor with a role in the anti-inflammatory response. *Ann Med.* 2004;36(5):347-54.
31. Bates JM, Flanagan K, Mo L, Ota N, Ding J, Ho S, et al. Dendritic cell CD83 homotypic interactions regulate inflammation and promote mucosal homeostasis. *Mucosal Immunol.* 2015;8(2):414-28.
32. Das T, Chen Z, Hendriks RW, and Kool M. A20/Tumor Necrosis Factor alpha-Induced Protein 3 in Immune Cells Controls Development of Autoinflammation and Autoimmunity: Lessons from Mouse Models. *Frontiers in immunology.* 2018;9:104.
33. Nimmerjahn F, and Ravetch JV. Fcgamma receptors as regulators of immune responses. *Nature reviews Immunology.* 2008;8(1):34-47.
34. Monteiro RC, and Van De Winkel JG. IgA Fc receptors. *Annual review of immunology.* 2003;21:177-204.
35. Huysamen C, and Brown GD. The fungal pattern recognition receptor, Dectin-1, and the associated cluster of C-type lectin-like receptors. *FEMS Microbiol Lett.* 2009;290(2):121-8.
36. McCormick SM, and Heller NM. Commentary: IL-4 and IL-13 receptors and signaling. *Cytokine.* 2015;75(1):38-50.
37. Ward AC. The role of the granulocyte colony-stimulating factor receptor (G-CSF-R) in disease. *Front Biosci.* 2007;12:608-18.
38. Dahlgren C, Holdfeldt A, Lind S, Martensson J, Gabl M, Bjorkman L, et al. Neutrophil Signaling That Challenges Dogmata of G Protein-Coupled Receptor Regulated Functions. *ACS Pharmacol Transl Sci.* 2020;3(2):203-20.
39. Zhao Y, and Shao F. The NAIP-NLRC4 inflammasome in innate immune detection of bacterial flagellin and type III secretion apparatus. *Immunol Rev.* 2015;265(1):85-102.
40. Gout E, Garlatti V, Smith DF, Lacroix M, Dumestre-Perard C, Lunardi T, et al. Carbohydrate recognition properties of human ficolins: glycan array screening reveals the sialic acid binding specificity of M-ficolin. *J Biol Chem.* 2010;285(9):6612-22.
41. Furukawa A, Kamishikiryo J, Mori D, Toyonaga K, Okabe Y, Toji A, et al. Structural analysis for glycolipid recognition by the C-type lectins Mincle and MCL. *Proc Natl Acad Sci U S A.* 2013;110(43):17438-43.
42. Freeman GJ, Long AJ, Iwai Y, Bourque K, Chernova T, Nishimura H, et al. Engagement of the PD-1 immunoinhibitory receptor by a novel B7 family member leads to negative regulation of lymphocyte activation. *The Journal of experimental medicine.* 2000;192(7):1027-34.
43. Asosingh K, Lauruschkat CD, Alemagno M, Frimel M, Wanner N, Weiss K, et al. Arginine metabolic control of airway inflammation. *JCI Insight.* 2020;5(2).
44. McGovern N, Shin A, Low G, Low D, Duan K, Yao LJ, et al. Human fetal dendritic cells promote prenatal T-cell immune suppression through arginase-2. *Nature.* 2017;546(7660):662-6.

45. Geiger R, Rieckmann JC, Wolf T, Basso C, Feng Y, Fuhrer T, et al. L-Arginine Modulates T Cell Metabolism and Enhances Survival and Anti-tumor Activity. *Cell.* 2016;167(3):829-42 e13.
46. Dowling JK, Afzal R, Gearing LJ, Cervantes-Silva MP, Annett S, Davis GM, et al. Mitochondrial arginase-2 is essential for IL-10 metabolic reprogramming of inflammatory macrophages. *Nat Commun.* 2021;12(1):1460.
47. Normand S, Waldschmitt N, Neerincx A, Martinez-Torres RJ, Chauvin C, Couturier-Maillard A, et al. Proteasomal degradation of NOD2 by NLRP12 in monocytes promotes bacterial tolerance and colonization by enteropathogens. *Nat Commun.* 2018;9(1):5338.
48. Ohira T, Arita M, Omori K, Recchiuti A, Van Dyke TE, and Serhan CN. Resolvin E1 receptor activation signals phosphorylation and phagocytosis. *J Biol Chem.* 2010;285(5):3451-61.
49. Heinrich PC, Behrmann I, Muller-Newen G, Schaper F, and Graeve L. Interleukin-6-type cytokine signalling through the gp130/Jak/STAT pathway. *Biochem J.* 1998;334 (Pt 2):297-314.
50. Bainbridge TW, DeAlmeida VI, Izrael-Tomasevic A, Chalouni C, Pan B, Goldsmith J, et al. Evolutionary divergence in the catalytic activity of the CAM-1, ROR1 and ROR2 kinase domains. *PLoS One.* 2014;9(7):e102695.
51. Eissmann P, Beauchamp L, Wooters J, Tilton JC, Long EO, and Watzl C. Molecular basis for positive and negative signaling by the natural killer cell receptor 2B4 (CD244). *Blood.* 2005;105(12):4722-9.
52. Caminschi I, Proietto AI, Ahmet F, Kitsoulis S, Shin Teh J, Lo JC, et al. The dendritic cell subtype-restricted C-type lectin Clec9A is a target for vaccine enhancement. *Blood.* 2008;112(8):3264-73.
53. Cueto FJ, Del Fresno C, and Sancho D. DNGR-1, a Dendritic Cell-Specific Sensor of Tissue Damage That Dually Modulates Immunity and Inflammation. *Frontiers in immunology.* 2019;10:3146.
54. Hwangbo C, Tae N, Lee S, Kim O, Park OK, Kim J, et al. Syntenin regulates TGF-beta1-induced Smad activation and the epithelial-to-mesenchymal transition by inhibiting caveolin-mediated TGF-beta type I receptor internalization. *Oncogene.* 2016;35(3):389-401.
55. Jura J, Skalniak L, and Koj A. Monocyte chemotactic protein-1-induced protein-1 (MCPIP1) is a novel multifunctional modulator of inflammatory reactions. *Biochim Biophys Acta.* 2012;1823(10):1905-13.
56. Adada MM, Orr-Gandy KA, Snider AJ, Canals D, Hannun YA, Obeid LM, et al. Sphingosine kinase 1 regulates tumor necrosis factor-mediated RANTES induction through p38 mitogen-activated protein kinase but independently of nuclear factor kappaB activation. *J Biol Chem.* 2013;288(38):27667-79.
57. Sugimoto T, Morioka N, Zhang FF, Sato K, Abe H, Hisaoka-Nakashima K, et al. Clock gene Per1 regulates the production of CCL2 and interleukin-6 through p38, JNK1 and NF-kappaB activation in spinal astrocytes. *Mol Cell Neurosci.* 2014;59:37-46.
58. Finlay D, and Cantrell D. The coordination of T-cell function by serine/threonine kinases. *Cold Spring Harb Perspect Biol.* 2011;3(1):a002261.
59. Lynch L. Adipose invariant natural killer T cells. *Immunology.* 2014;142(3):337-46.

60. Gaya M, Barral P, Burbage M, Aggarwal S, Montaner B, Warren Navia A, et al. Initiation of Antiviral B Cell Immunity Relies on Innate Signals from Spatially Positioned NKT Cells. *Cell.* 2018;172(3):517-33 e20.
61. Lee YJ, Wang H, Starrett GJ, Phuong V, Jameson SC, and Hogquist KA. Tissue-Specific Distribution of iNKT Cells Impacts Their Cytokine Response. *Immunity.* 2015;43(3):566-78.
62. Fernandez CS, Jegaskanda S, Godfrey DI, and Kent SJ. In-vivo stimulation of macaque natural killer T cells with alpha-galactosylceramide. *Clinical and experimental immunology.* 2013;173(3):480-92.
63. Bricard G, Venkataswamy MM, Yu KO, Im JS, Ndonye RM, Howell AR, et al. A-galactosylceramide analogs with weak agonist activity for human iNKT cells define new candidate anti-inflammatory agents. *PLoS One.* 2010;5(12):e14374.
64. Giaccone G, Punt CJ, Ando Y, Ruijter R, Nishi N, Peters M, et al. A phase I study of the natural killer T-cell ligand alpha-galactosylceramide (KRN7000) in patients with solid tumors. *Clinical cancer research : an official journal of the American Association for Cancer Research.* 2002;8(12):3702-9.
65. Woltman AM, Ter Borg MJ, Binda RS, Sprengers D, von Blomberg BM, Scheper RJ, et al. Alpha-galactosylceramide in chronic hepatitis B infection: results from a randomized placebo-controlled Phase I/II trial. *Antiviral therapy.* 2009;14(6):809-18.
66. Saltiel AR, and Olefsky JM. Inflammatory mechanisms linking obesity and metabolic disease. *The Journal of clinical investigation.* 2017;127(1):1-4.
67. Damouche A, Lazure T, Avettand-Fènoël V, Huot N, Dejucq-Rainsford N, Satie AP, et al. Adipose Tissue Is a Neglected Viral Reservoir and an Inflammatory Site during Chronic HIV and SIV Infection. *PLoS pathogens.* 2015;11(9):e1005153.
68. Liu Y, Beyer A, and Aebersold R. On the Dependency of Cellular Protein Levels on mRNA Abundance. *Cell.* 2016;165(3):535-50.
69. Kato Y, Zaid A, Davey GM, Mueller SN, Nutt SL, Zotos D, et al. Targeting Antigen to Clec9A Primes Follicular Th Cell Memory Responses Capable of Robust Recall. *J Immunol.* 2015;195(3):1006-14.
70. Fullerton JN, and Gilroy DW. Resolution of inflammation: a new therapeutic frontier. *Nat Rev Drug Discov.* 2016;15(8):551-67.
71. Truneh AC, FJ; Jones, TJ; Gresgson, JP. In: Office USP ed. USA: NKT Therapuetics; 2013.
72. Exley MA, Hou R, Shaulov A, Tonti E, Dellabona P, Casorati G, et al. Selective activation, expansion, and monitoring of human iNKT cells with a monoclonal antibody specific for the TCR alpha-chain CDR3 loop. *European journal of immunology.* 2008;38(6):1756-66.
73. . FastQC: A quality control tool for high throughput sequence data. http://www.bioinformatics.babraham.ac.uk/projects/fastqc/. Accessed 10/09/2020, 2020.
74. Bolger AM, Lohse M, and Usadel B. Trimmomatic: a flexible trimmer for Illumina sequence data. *Bioinformatics.* 2014;30(15):2114-20.
75. Schmieder R, and Edwards R. Quality control and preprocessing of metagenomic datasets. *Bioinformatics.* 2011;27(6):863-4.

960 76. Kim D, Pertea G, Trapnell C, Pimentel H, Kelley R, and Salzberg SL. TopHat2: accurate
961 alignment of transcriptomes in the presence of insertions, deletions and gene fusions.
962 *Genome Biol.* 2013;14(4):R36.
963 77. Dobin A, Davis CA, Schlesinger F, Drenkow J, Zaleski C, Jha S, et al. STAR: ultrafast
964 universal RNA-seq aligner. *Bioinformatics.* 2013;29(1):15-21.
965 78. O'Leary NA, Wright MW, Brister JR, Ciufo S, Haddad D, McVeigh R, et al. Reference
966 sequence (RefSeq) database at NCBI: current status, taxonomic expansion, and
967 functional annotation. *Nucleic Acids Res.* 2016;44(D1):D733-45.
968 79. Anders S, and Huber W. Differential expression analysis for sequence count data.
969 *Genome Biol.* 2010;11(10):R106.
970 80. Robinson MD, McCarthy DJ, and Smyth GK. edgeR: a Bioconductor package for
971 differential expression analysis of digital gene expression data. *Bioinformatics.*
972 2010;26(1):139-40.
973 81. Kolde R. pheatmap: Pretty Heatmaps. https://CRAN.R-project.org/package=pheatmap.
974 82. Roederer M, Nozzi JL, and Nason MC. SPICE: exploration and analysis of post-cytometric
975 complex multivariate datasets. *Cytometry A.* 2011;79(2):167-74.

976

977

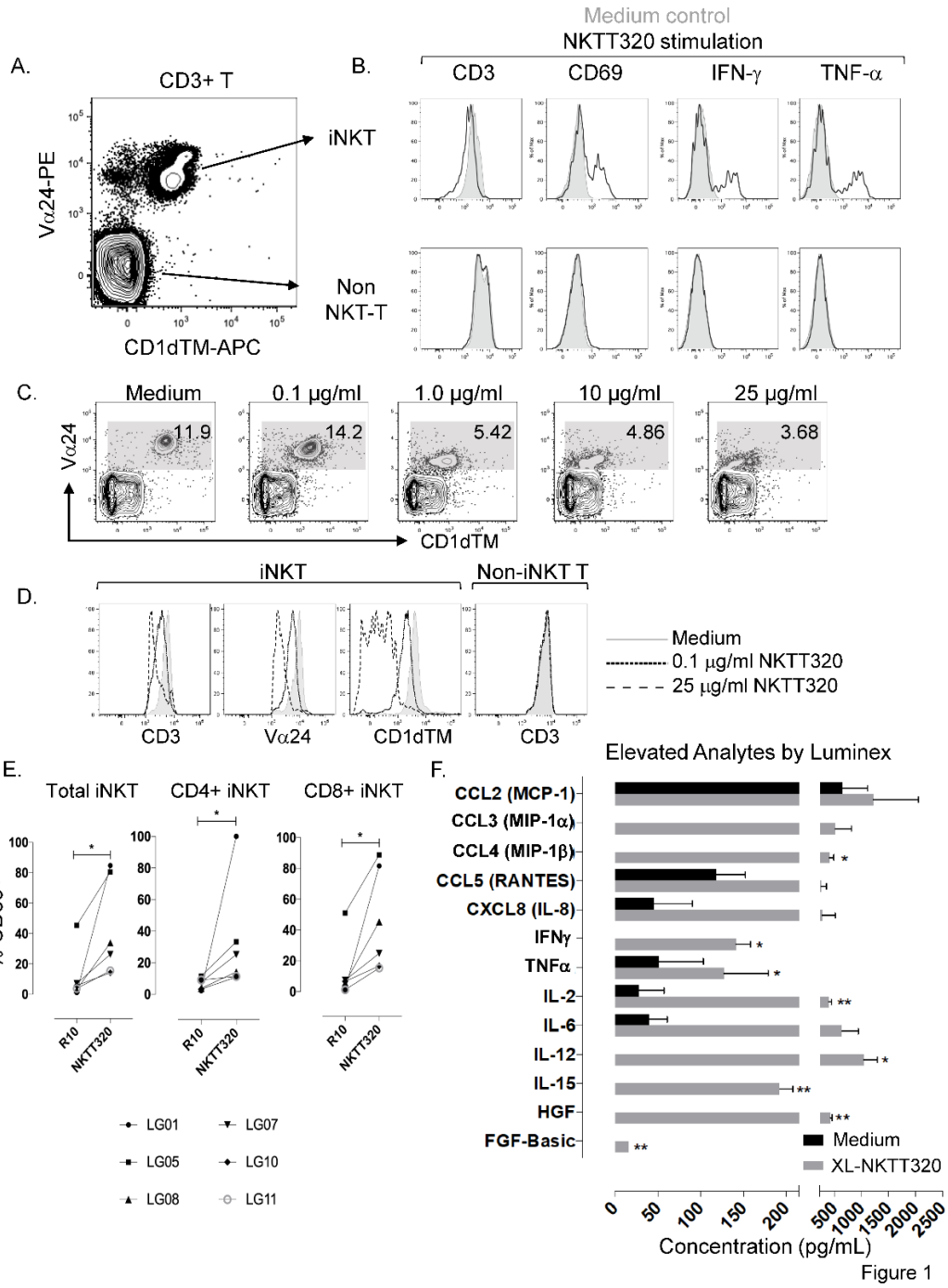

Figure 1

Figure 1. iNKTs are specifically activated by NKTT320.

(A) Representative plot showing iNKT and non-NKT T-cell gating strategy gated on CD3+ T-cells. (B) Overlay histograms (unstimulated=shaded, NKTT320=open histogram) comparing CD3, CD69 and cytokine expression on R10 and NKTT320 (200ng/mL) treated PBMCs stimulated for 4hrs *in vitro*, iNKTs (top) and non-NKT T–cells (bottom). (C-D) *In vitro* data showing iNKT frequency and TCR downregulation after overnight incubation with escalating concentrations of NKTT320. TCR downregulation is measured by Vα24, CD1d and CD3. (E) CD4+ and CD8+ iNKT activation *in vitro* measured by CD69 in 6 animals stimulated with 200ng/mL NKTT320 for 4 hours. (F) Luminex data showing analytes which were elevated in cells stimulated with 200ng/mL NKTT320 compared to medium. Supernatants were collected after 48 hours. Statistics were done by non-parametric Wilcoxon signed-rank test (n=3). *<0.05, **<0.01.

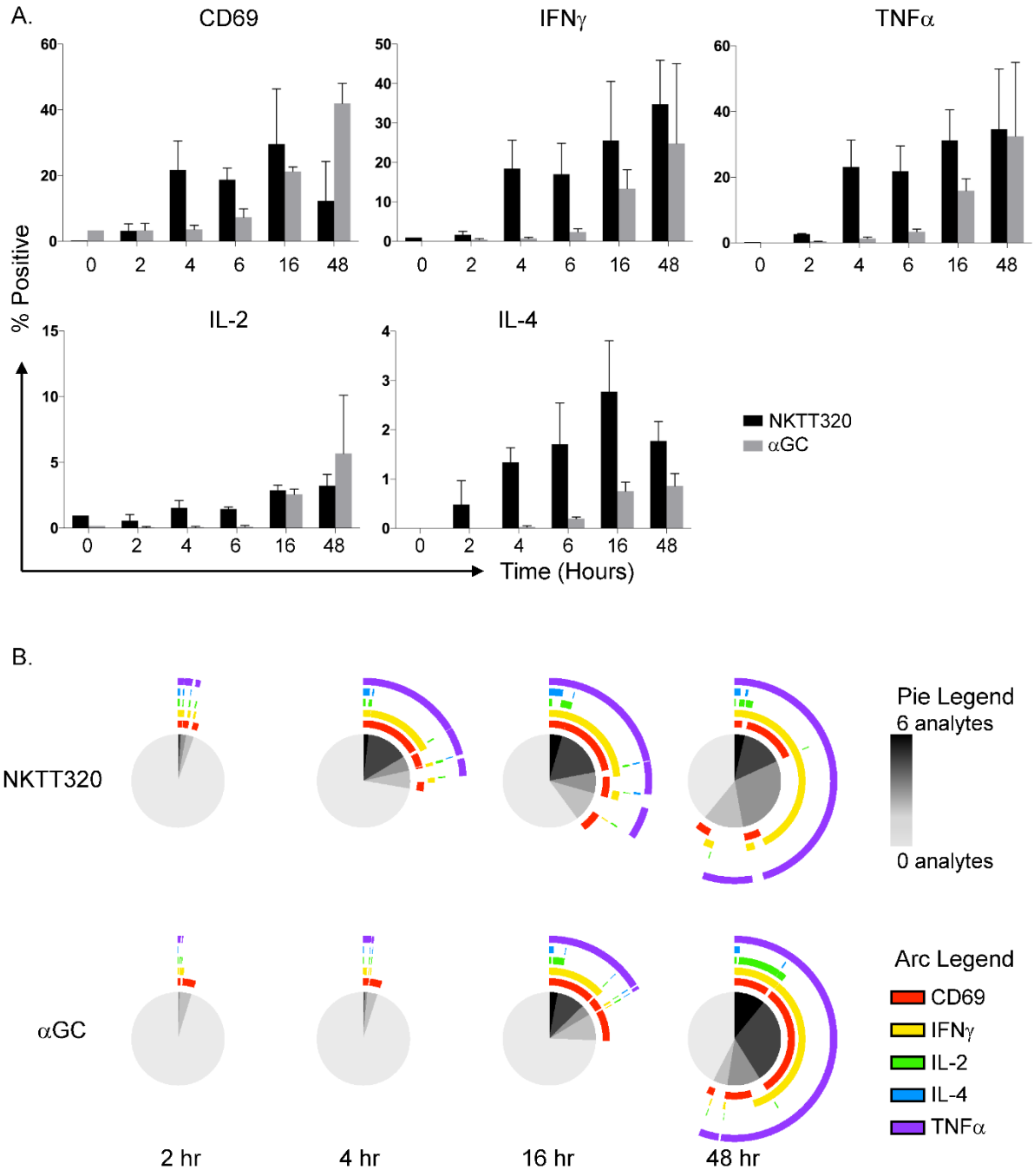

Figure 2. Differential kinetics of NKTT320 and aGC activation *in vitro*.
(A) Intracellular cytokine staining of PBMCs stimulated with goat-anti-mouse-IgG cross-linked NKTT320 or αGC loaded on C1Rd cells, harvested and stained at 0, 2, 4, 6, 16, and 48 hours. Data on cytokine secretion gated on iNKT cells. Mean and SEM shown (n=2). (B) SPICE analysis of experiment described in (A) showing kinetic differences in speed, magnitude and co-expression of cytokines in NKTT320 and αGC stimulated iNKT cells (n=2).

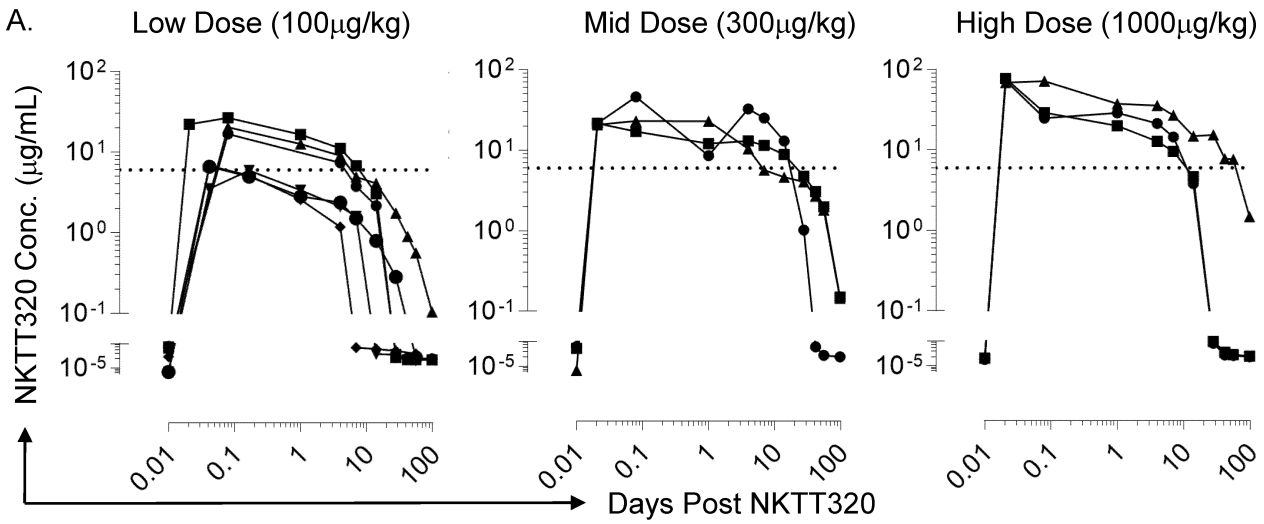

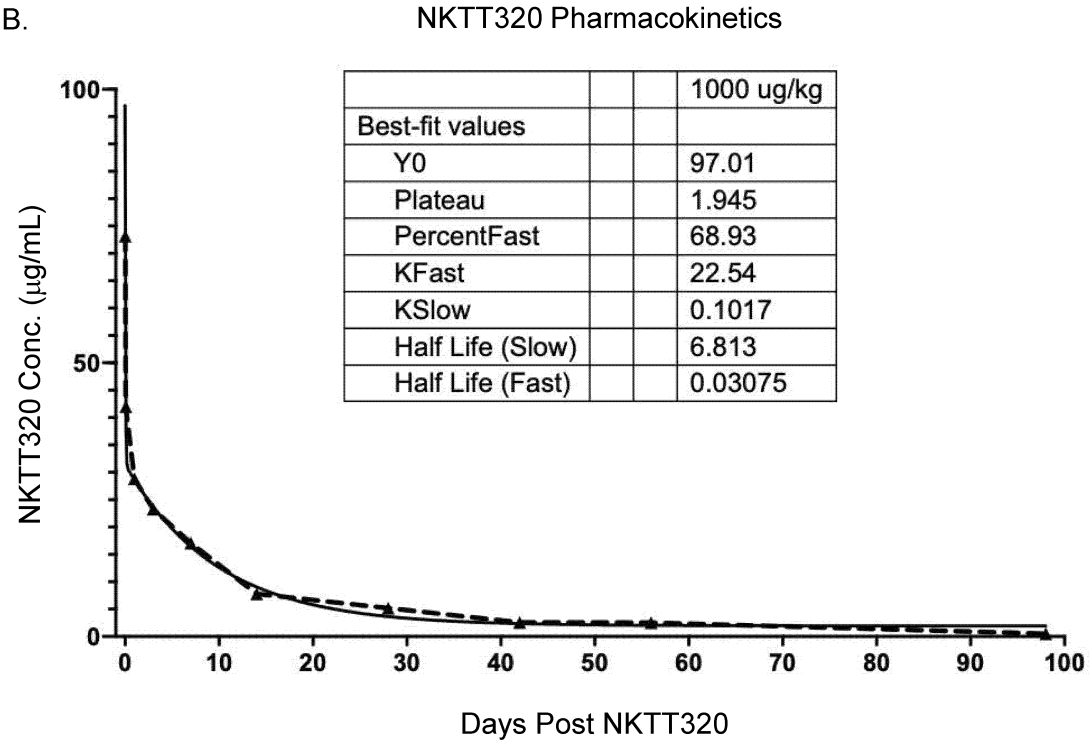

			1000 ug/kg
Best-fit values			
Y0			97.01
Plateau			1.945
PercentFast			68.93
KFast			22.54
KSlow			0.1017
Half Life (Slow)			6.813
Half Life (Fast)			0.03075

Figure 3. *In vivo* pharmacokinetics of NKTT320.
(A) plasma NKTT320 concentration measured by ELISA in animals that received Low (100ug/kg, n=5), Mid (300ug/kg, n=3) and High (1000ug/kg, n=3) doses of NKTT320 IV. Horizontal dotted line shows NKT TCR saturation level (6ug/mL). Samples were taken at day 0 and 30 minutes, 2 hours, day 1, 4, 7, 14, 28, 42, 56, and 98 post-NKTT320 treatment. (B) NKTT320 pharmacokinetic data determined by a single dose of 1000ug/kg. Half-life shown in days.

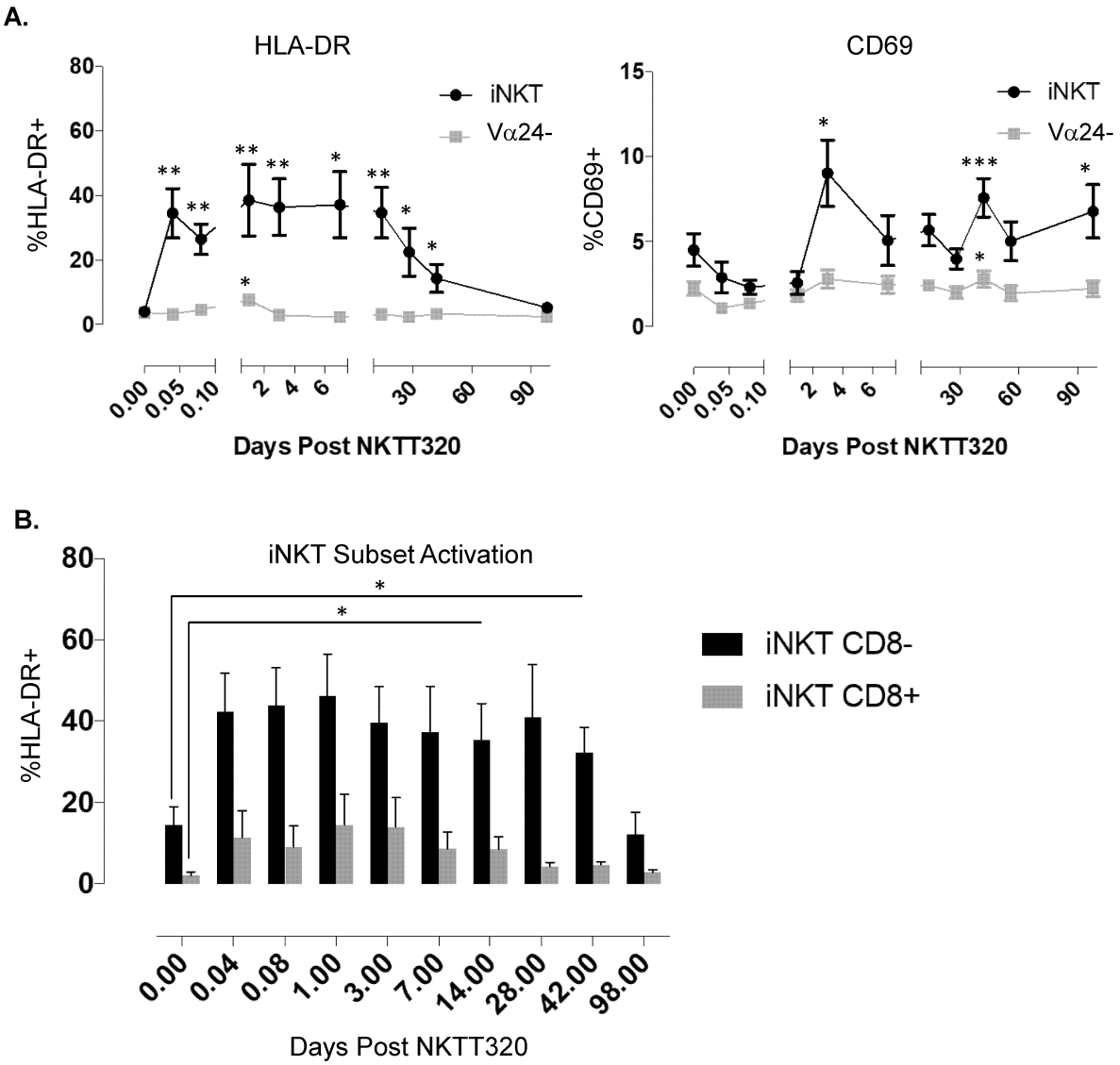

Figure 4. iNKT activation after *in vivo* NKTT320 treatment.
(A) Mean HLA-DR and CD69 expression in iNKT versus non-iNKT-T. (B) iNKT CD8- vs iNKT CD8+ in animals treated *in vivo* with NKTT320 (n=9). Paired t-tests were used to determine statistical significance of increased activation of total iNKT or Va24- T (A), and CD8+ or CD8- iNKT (B) compared to their respective baseline values. * <0.05.

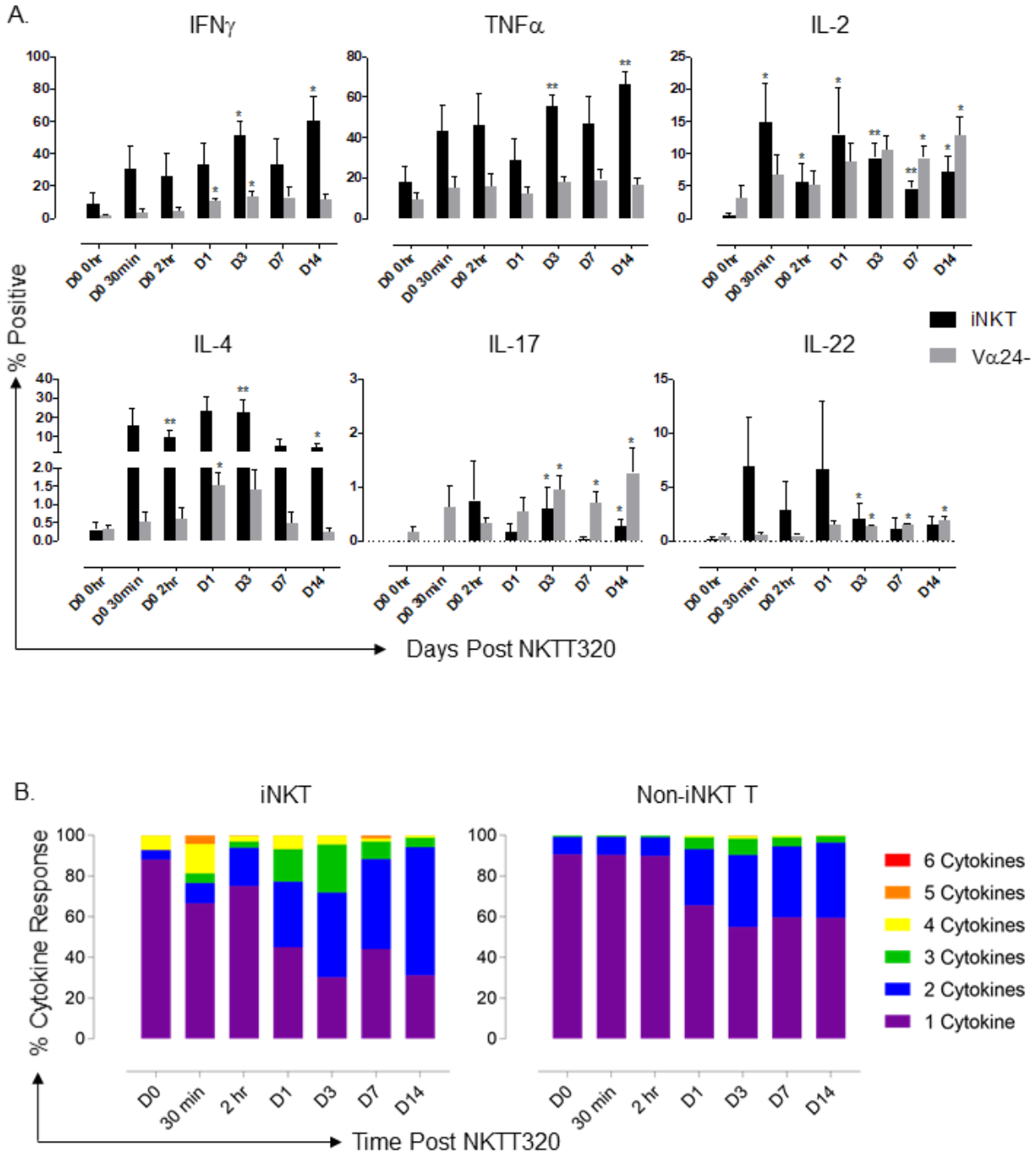

Fig. 5. NKTT320 rapidly induces functional changes in T-cell subsets.
(A) Mean cytokine expression in iNKTs and Non-iNKT Ts measured by intracellular cytokine staining following overnight PMA/ionomycin stimulation. Samples were taken at day 0 and 30 minutes, 2 hours, day 1, 4, 7, 14. Data in n=7 MCM. Significance compared to baseline is indicated by an asterisk and was determined by paired parametric t-test. *<0.05, **<0.01. (B) Proportion of iNKT vs Non-iNKT T-cells responding with one or more cytokines after stimulation with PMA/ionomycin (n=7).

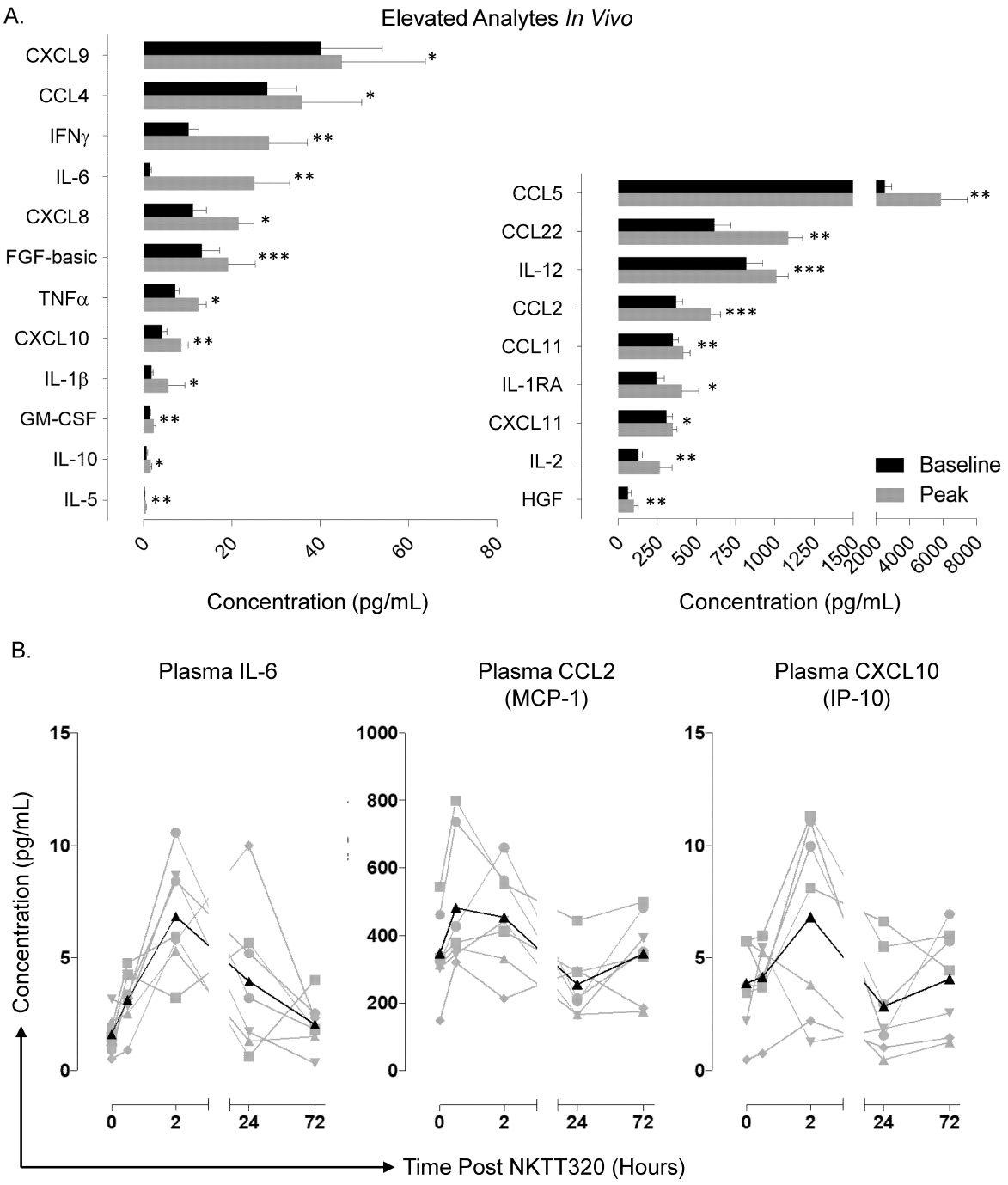

Fig. 6. NKTT320 rapidly induces functional changes *in vivo*.
(A) Analytes significantly upregulated after NKTT320 treatment *in vivo* measured by plasma Luminex at baseline and peak (n=12). *<0.05, **<0.01, ***<0.001.(B) *Ex vivo* plasma Luminex kinetics post NKTT320 for IL-6, CCL2, and CXCL10 in 7 animals from a single Luminex run.

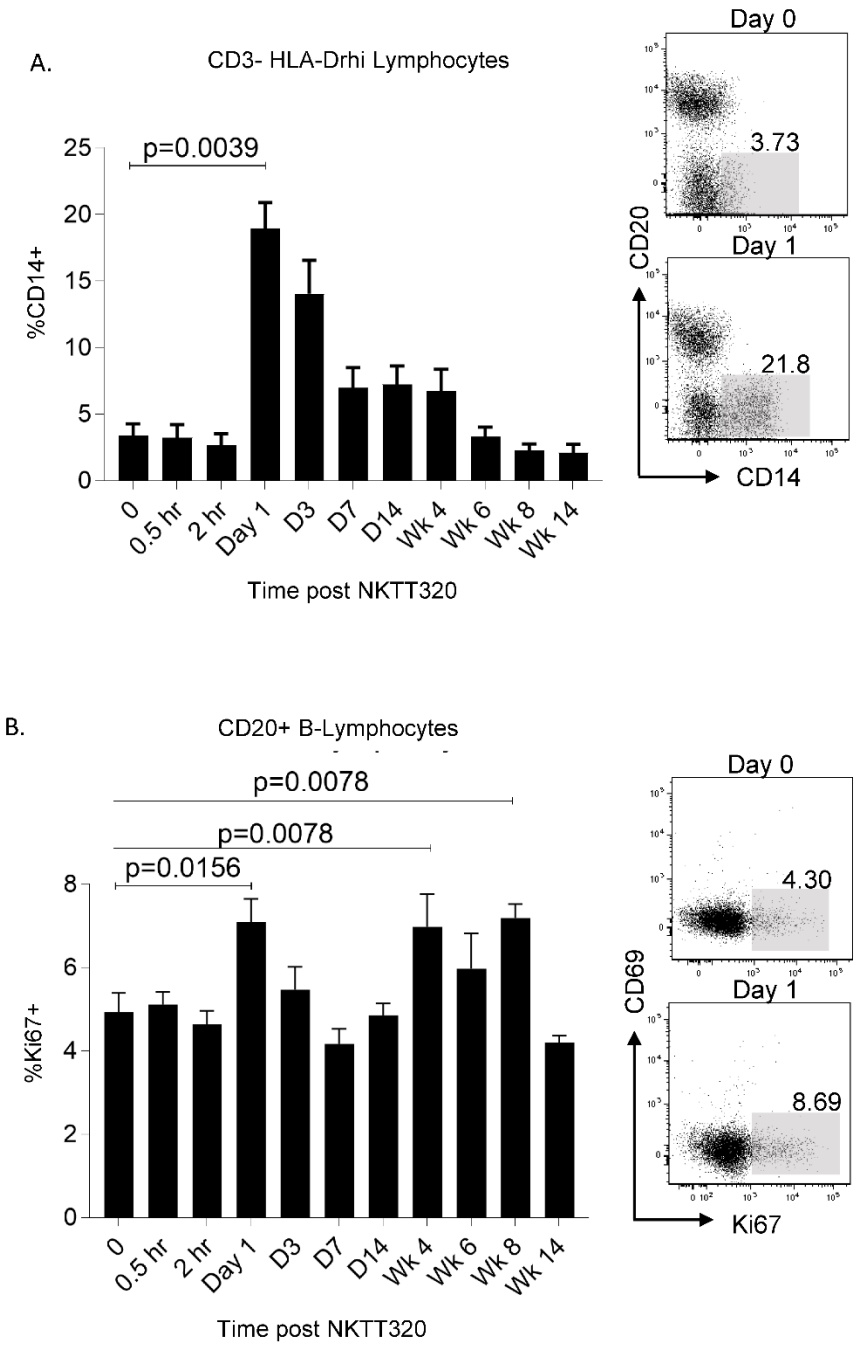

Fig. 7. Increased frequency of circulating monocytes and increased proliferation of B-lymphocytes after NKTT320.

(A) Monocyte frequency shown as percentage of CD3- HLA-DRhi lymphocytes. Representative plots show an increase in circulating monocytes on day 1 compared to day 0. (B) B-cell proliferation measured by Ki67 expression on CD20+ B-cells. Representative plots show increases in B-cell Ki67 expression at day 1 post NKTT320 administration. Significant differences from baseline were determined through non-parametric Wilcoxon signed-rank test (n=9 MCM).

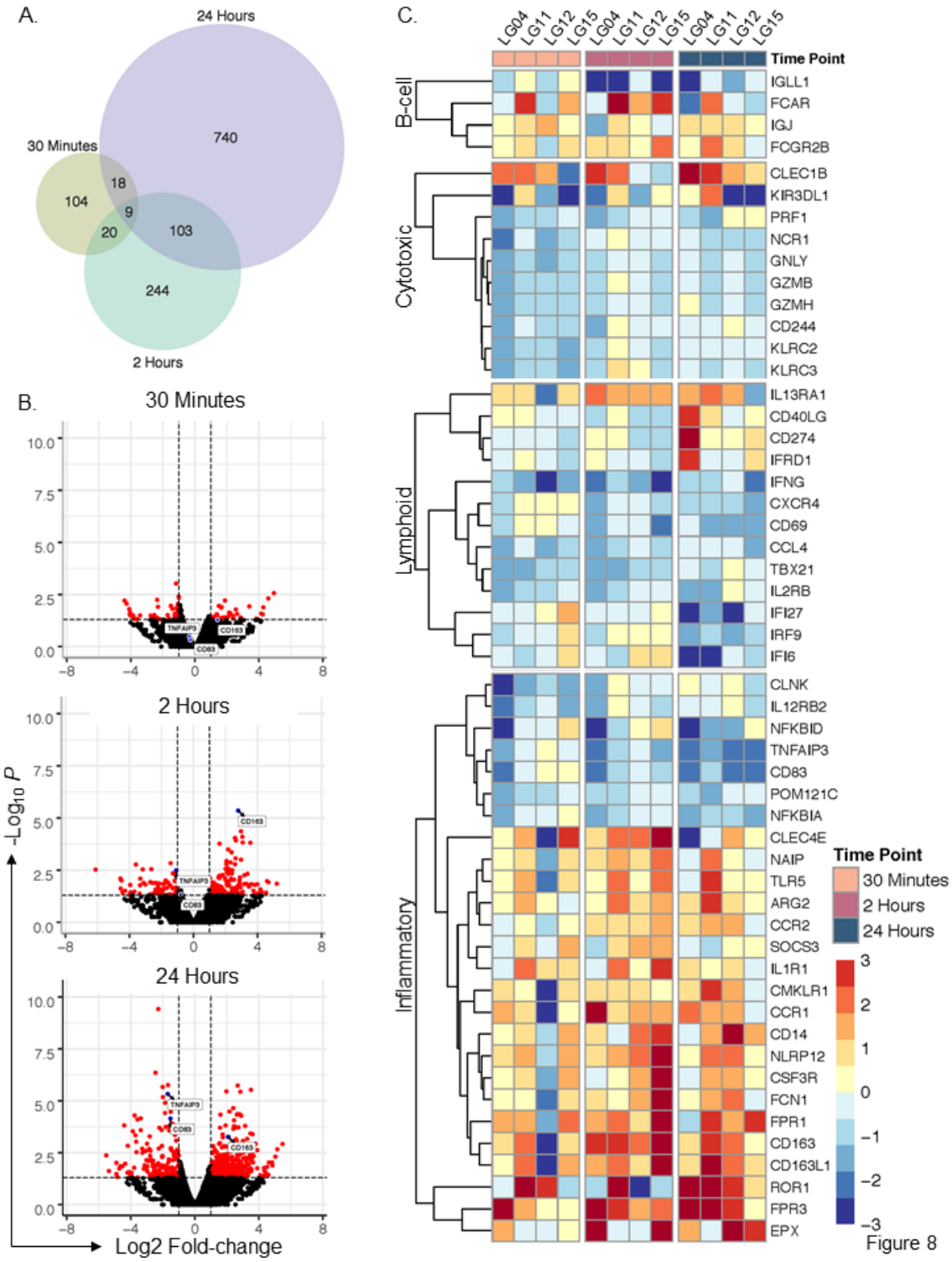

Figure 8

Fig. 8. RNA-seq analysis reveals rapid differential gene expression

A) Venn diagram showing differentially expressed genes where p-value <0.05 at 30 minutes, 2 hours and 24 hours. (B) Volcano plots of all genes showing kinetic increases in transcriptomic changes over time. (C) Heatmaps showing differential expression (log_2 fold change) for targeted genes where p-value <.05 related to B-cell, cytotoxic, lymphoid and inflammatory pathways.

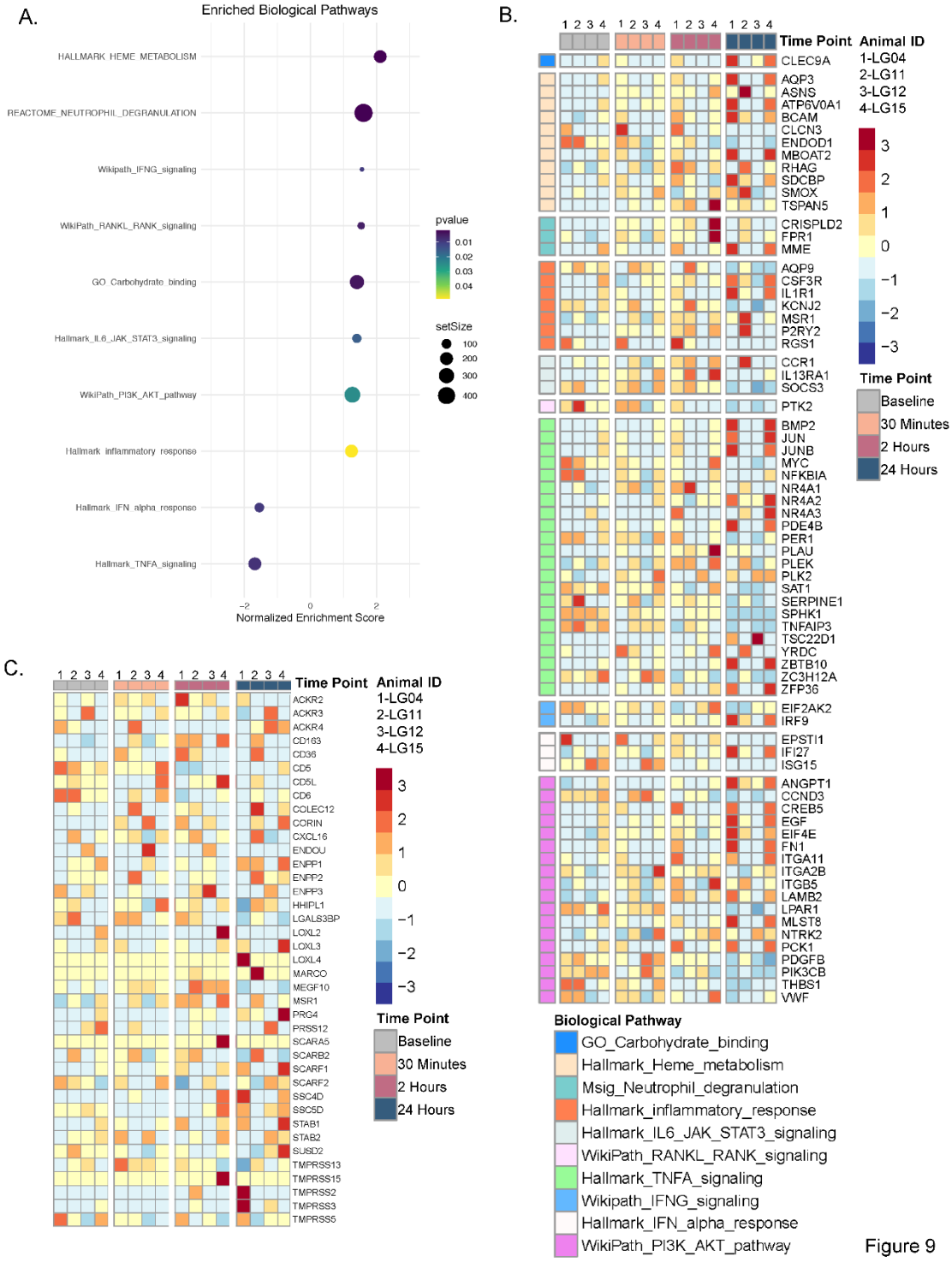

Figure 9

Figure 9. Biological pathways related to NK T cells are enriched upon anti-NKT antibody administration. (A). Normalized enrichment scores (NES) of relevant NKT-related pathways selected from an unbiased gene set enrichment analysis (GSEA). Color ramp represents NES significance defined by a Fisher's Exact test. Dot size represents 'setSize', or number of genes contained within an *a priori*-defined biological pathway. (B) Composite heatmap of genes meeting a significance threshold ($p < 0.05$) at 30 minute-, 2 hour-, and 1 day-post NKT-antibody administration that are contained within significantly enriched pathways depicted in (A). Rows are scaled by z-score-normalized expression. (C) Heatmap of genes within the GO pathway "scavenger receptor activity".

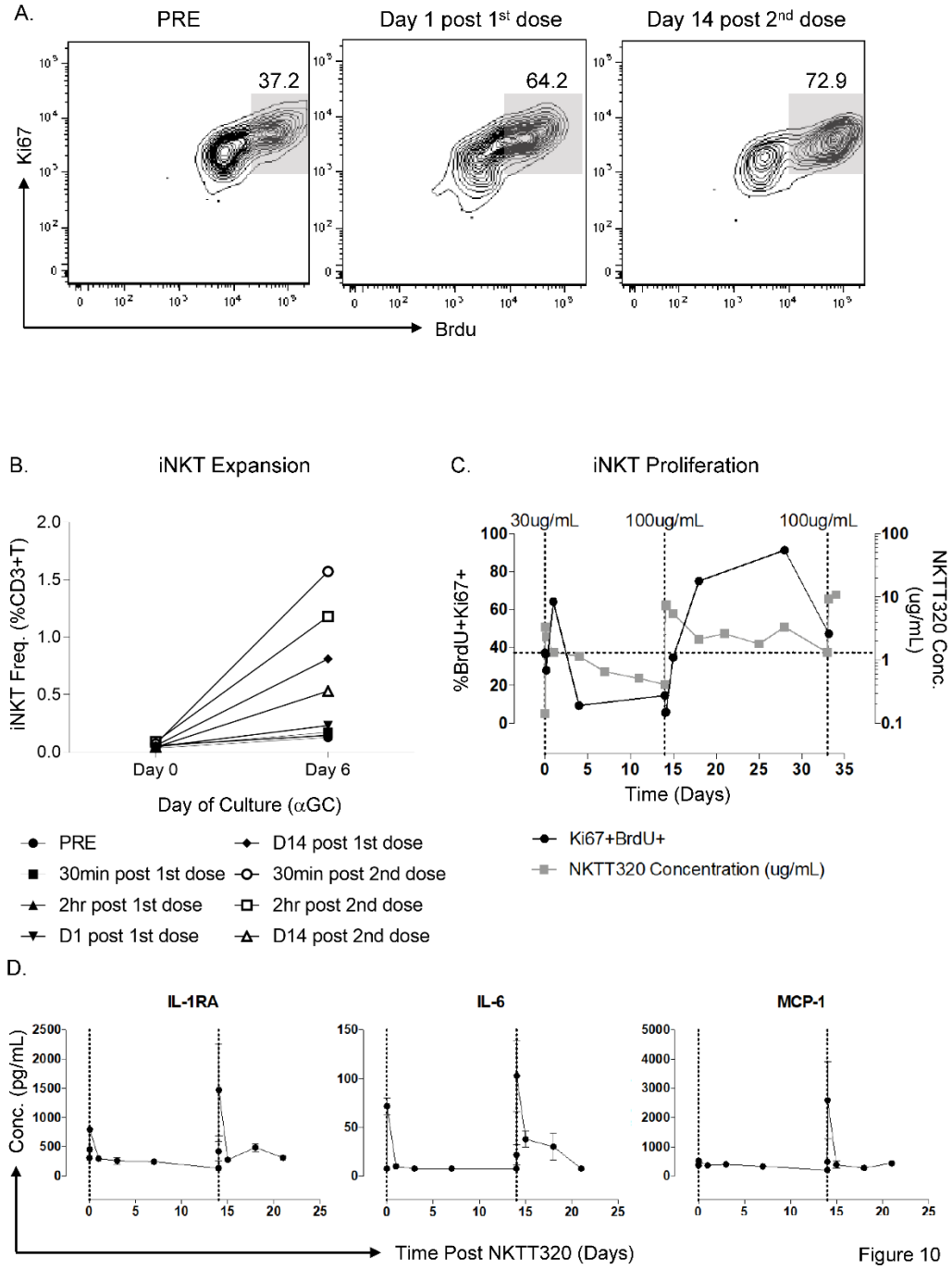

Figure 10

Fig. 10. iNKTs retain proliferative capacity after NKTT320 indicating a lack of NKT anergy.
(A) Representative plots of iNKT proliferative capacity after stimulation with aGC, pre-NKTT320, D1 post 1st dose and D14 post 2nd dose. Data from *in vitro* proliferation assays performed in 1 multiply dosed MCM. (B) iNKT expansion after 6-day culture with aGC at the following time points: pre-NKTT320, 30min, 2hr, D1 and D14 post 1st dose; and 30min, 2hr, and D14 post 2nd dose. Data from *in vitro* proliferation assays performed in 1 multiply dosed MCM. (C) iNKT proliferation measured as BrdU+ Ki67+ double positives by flow cytometry. Proliferation data is compared to plasma NKTT320 concentration measured by NKTT320 ELISA. Vertical lines indicate the time and concentration of each dose. Horizontal line indicates baseline iNKT proliferation. Vertical lines indicate timing of dosing. (D) *Ex vivo* plasma luminex data from animals that received 2 doses of NKTT320 (n=4).

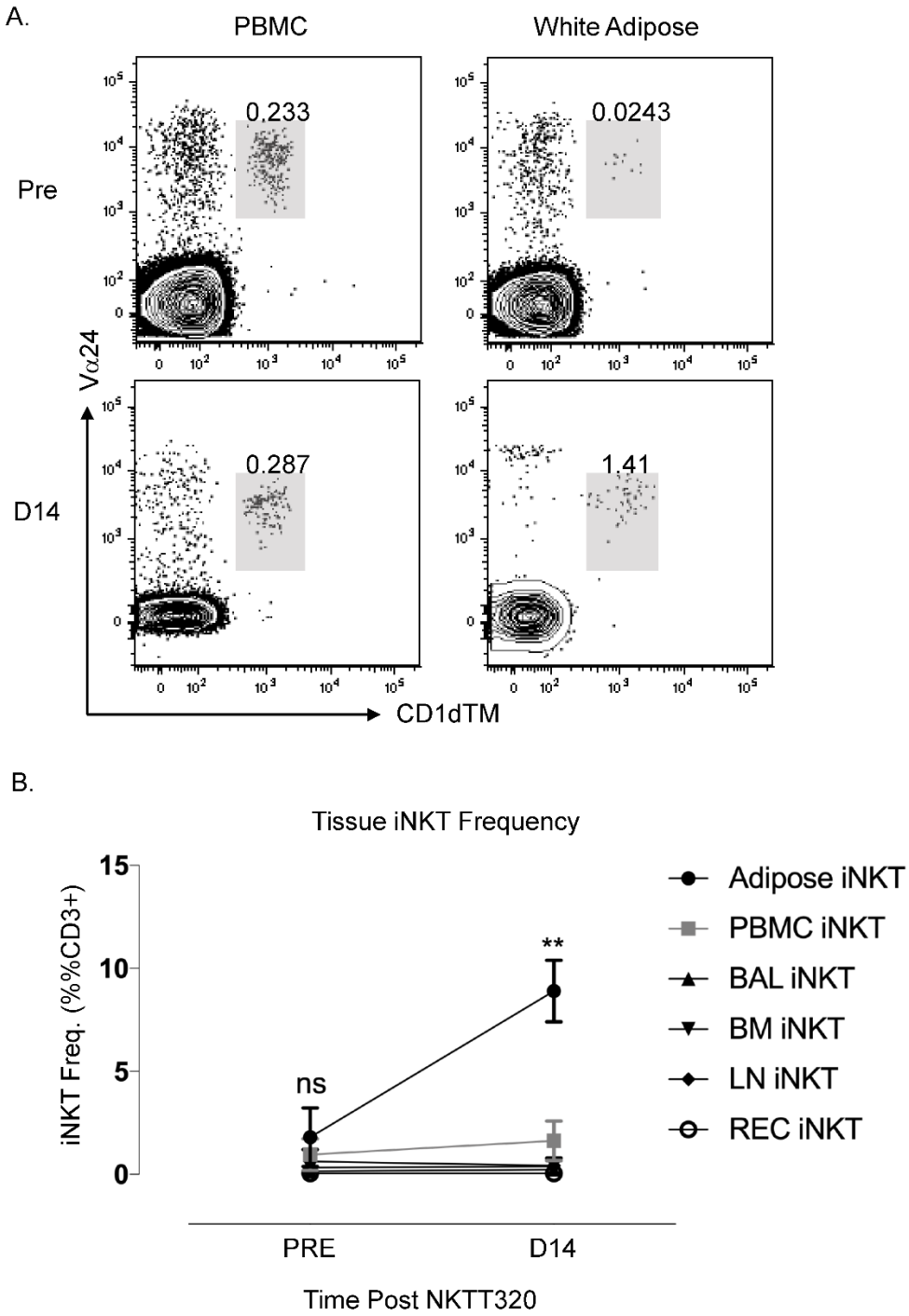

Fig. 11. NKTT320 treatment *in vivo* results in trafficking of iNKTs to adipose tissue sites.
(A) Representative plots of iNKT frequency pre and post NKTT320 treatment in white adipose and PBMC. (B) iNKT frequency in tissues and PBMC pre and 14 days post NKTT320 treatment (n=3). Paired t-test, **<0.01. 'BAL'-bronchoalveolar lavage; 'BM'-bone marrow; 'LN'-lymph node; 'REC'-rectal mucosa.

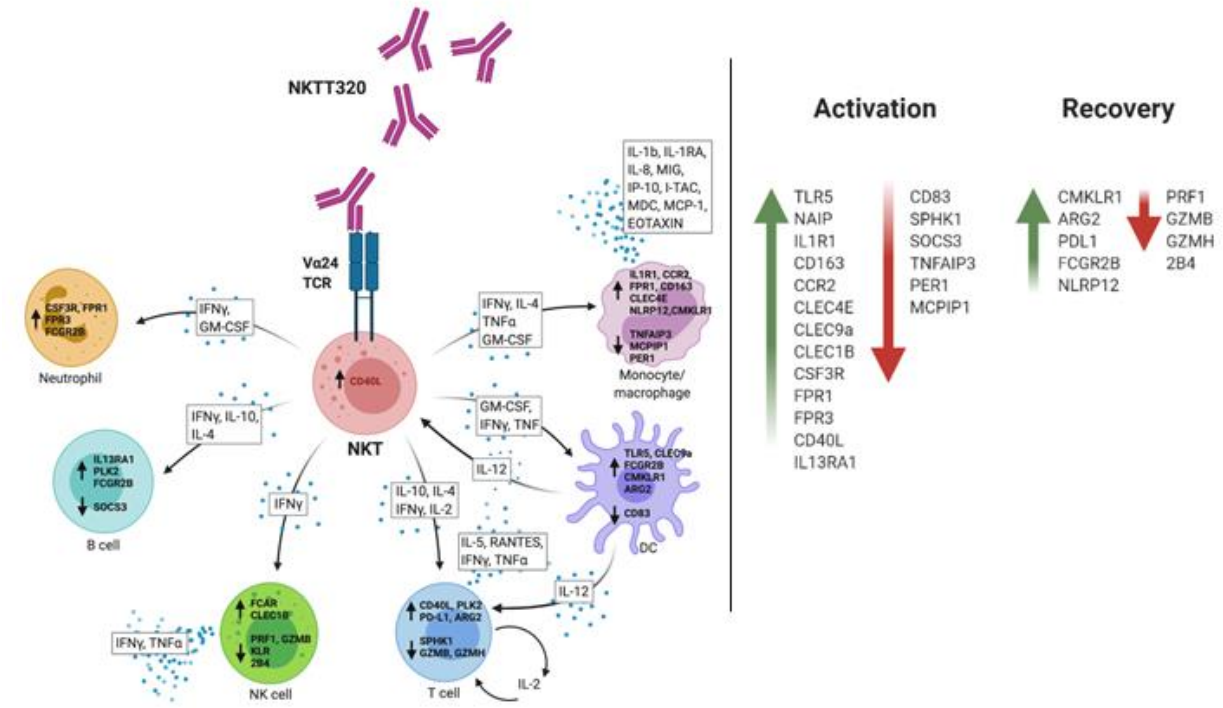

Fig. 12. NKTT320 immune modulation.
Schematic effect of NKTT320 on iNKT and downstream immune cell subsets as measured by Luminex, ICS, and RNA-Seq. Genes and secreted molecules are placed according to potential cellular sources.